Evaluating the segmented post-rift stratigraphic architecture of the Guyanas continental margin

Max Casson, Jason Jeremiah, Gérôme Calvès, Frédéric de Ville de Goyet, Kyle Reuber, Mike Bidgood, Daniela Reháková, Luc Bulot, Jonathan Redfern

▶ **To cite this version:**

Max Casson, Jason Jeremiah, Gérôme Calvès, Frédéric de Ville de Goyet, Kyle Reuber, et al.. Evaluating the segmented post-rift stratigraphic architecture of the Guyanas continental margin. Petroleum Geoscience, 2021, 27 (3), ⟨10.1144/petgeo2020-099⟩. ⟨hal-03128117⟩

HAL Id: hal-03128117

https://hal.science/hal-03128117v1

Submitted on 23 Feb 2021

HAL is a multi-disciplinary open access archive for the deposit and dissemination of scientific research documents, whether they are published or not. The documents may come from teaching and research institutions in France or abroad, or from public or private research centers.

L'archive ouverte pluridisciplinaire **HAL**, est destinée au dépôt et à la diffusion de documents scientifiques de niveau recherche, publiés ou non, émanant des établissements d'enseignement et de recherche français ou étrangers, des laboratoires publics ou privés.

Copyright - All rights reserved

Downloaded from http://pg.lyellcollection.org/ at University of Manchester, The John Rylands University Library on February 1, 2021

Accepted Manuscript

Petroleum Geoscience

Evaluating the segmented post-rift stratigraphic architecture of the Guyanas continental margin

Max Casson, Jason Jeremiah, Gérôme Calvès, Frédéric de Ville de Goyet, Kyle Reuber, Mike Bidgood, Daniela Reháková, Luc Bulot & Jonathan Redfern

DOI: https://doi.org/10.1144/petgeo2020-099

To access the most recent version of this article, please click the DOI URL in the line above. When citing this article please include the above DOI.

Received 14 September 2020
Revised 8 January 2021
Accepted 23 January 2021

© 2021 The Author(s). Published by The Geological Society of London for GSL and EAGE. All rights reserved. For permissions: http://www.geolsoc.org.uk/permissions. Publishing disclaimer: www.geolsoc.org.uk/pub_ethics

Supplementary material at https://doi.org/10.6084/m9.figshare.c.5280490

Manuscript version: Accepted Manuscript
This is a PDF of an unedited manuscript that has been accepted for publication. The manuscript will undergo copyediting, typesetting and correction before it is published in its final form. Please note that during the production process errors may be discovered which could affect the content, and all legal disclaimers that apply to the journal pertain.

Although reasonable efforts have been made to obtain all necessary permissions from third parties to include their copyrighted content within this article, their full citation and copyright line may not be present in this Accepted Manuscript version. Before using any content from this article, please refer to the Version of Record once published for full citation and copyright details, as permissions may be required.

Downloaded from http://pg.lyellcollection.org/ at University of Manchester, The John Rylands University Library on February 1, 2021

Evaluating the segmented post-rift stratigraphic architecture of the Guyanas continental margin

Max Casson[1], Jason Jeremiah[2], Gérôme Calvès[3], Frédéric de Ville de Goyet[4], Kyle Reuber[5], Mike Bidgood[6], Daniela Reháková[7], Luc Bulot[8,1], Jonathan Redfern[1]

[1] North Africa Research Group (NARG), Department of Earth and Environmental Sciences, The University of Manchester, Williamson Building, Oxford Road, Manchester, M13 9PL, UK

CURRENT – Equinor ASA, Equinor Research Centre, Svanholmen 8, Forus, Norway

Email correspondence – mcass@equinor.com

[2] Golden Spike Geosolutions Ltd., 20 Ten Acres Crescent, Stevenage, Hertfordshire, SG2 9US, UK

[3] Université Toulouse 3, Paul Sabatier, Géosciences Environnement Toulouse, 14 avenue Edouard Belin, 31400, Toulouse, France

[4] PetroStrat Ltd. Tan-y-Graig, Parc Caer Seion, Conwy, LL32 8FA, Wales, UK

[5] ION GeoVentures, Houston, Texas, USA

[6] GSS (Geoscience) Ltd., 2 Meadows Drive, Oldmeldrum, Aberdeenshire, AB51 0GA, UK

[7] Comenius University in Bratislava, Faculty of Natural Sciences, Department of Geology and Paleontology, Mlynská dolina, Ilkovičova 6, 842 15 Bratislava, Slovakia

[8] Aix-Marseille Université, CNRS, IRD, Collège de France, INRA, Cerege, Site Saint-Charles, Case 67, 3, Place Victor Hugo, 13331, Marseille Cedex 3, *France*

ACCEPTED MANUSCRIPT

Downloaded from http://pg.lyellcollection.org/ at University of Manchester, The John Rylands University Library on February 1, 2021

Abstract

Segmentation of the Guyanas continental margin of South America is inherited from the dual-phase Mesozoic rifting history controlling the first-order post-rift sedimentary architecture. The margin is divided into two segments by a transform marginal plateau (TMP), the Demerara Rise, into the Central and Equatorial Atlantic domains. This paper investigates the heterogeneities in the post-rift sedimentary systems at a mega-regional scale (>1000 km). Re-sampling seven key exploration wells and scientific boreholes provides new data (189 analysed samples) that have been used to build a high-resolution stratigraphic framework using multiple biostratigraphic techniques integrated with organic geochemistry to refine the timing of 10 key stratigraphic surfaces and three megasequences. The results have been used to calibrate the interpretation of a margin-scale two-dimensional seismic reflection dataset and build megasequence isochore maps, structural restorations and gross depositional environment maps at key time intervals of the margin evolution.

Our findings revise the dating of the basal succession drilled by the A2-1 well, indicating that the oldest post-rift sequence penetrated along the margin is late Tithonian age (previously Callovian). Early Central Atlantic carbonate platform sediments passively infilled subcircular-shaped basement topography controlled by underlying basement structure of thinned continental crust. Barremian-Aptian rifting in the Equatorial Atlantic folding and thrusting the Demerara Rise resulting in major uplift, gravitational margin collapse, transpressional structures, and peneplanation of up to 1 km of sediment capped by the regional angular base Albian unconformity. Equatorial Atlantic rifting led to margin segmentation and the formation of the TMP, where two major unconformities developed during the intra Late Albian and base Cenomanian. These two unconformities are time synchronous with oceanic crust accretion offshore French Guiana and in the Demerara-Guinea transform, respectively. A marine connection between the Central and Equatorial Atlantic is demonstrated by middle Late Albian times, coinciding with deposition of the organic-rich source rock of the Canje Formation) (average TOC 4.21 %). The succession is variably truncated by the middle Campanian unconformity. Refining the stratigraphic framework within the context of the structural evolution and segmentation of the Guyanas margin impacts the understanding of key petroleum system elements.

Key words: stratigraphy; post-rift; continental margins; Mesozoic; Demerara Rise; Central Atlantic

ACCEPTED MANUSCRIPT

Downloaded from http://pg.lyellcollection.org/ at University of Manchester, The John Rylands University Library on February 1, 2021

Introduction

Continental margins are heterogeneous at various scales, resulting in along strike asymmetry and segmentation. First-order structural and tectonic segmentation is mainly related to pre-existing basement heterogeneity often separated by long-lived weaknesses in the continental crust. Subsequently modified by the rifting process, i.e. the magnitude and orientation of extension (β-factor; McKenzie, 1978), and breakup magmatism, volcanic versus non-volcanic margins (Franke, 2013). Post-rift passive margin subsidence and sedimentation finally influences the overall margin architecture, but it is still largely controlled by the pre-existing structure and thermal subsidence (Clemson et al., 1997). Old segmented continental margins, and particularly marginal plateaus record multiple rift-to-drift cycles and/or failed rifts related to the gradual fragmentation of supercontinents (Wilson cycle; Wilson, 1966; Burke & Dewey, 1974). Exemplified in the studied Guyanas continental margin of South America, caused by the opening of the Central Atlantic and succeeding transform-dominated Equatorial Atlantic, with oblique opening directions (Fig. 1A; Reuber et al., 2016). Conventional models of lithospheric thinning assume continuous post-rift subsidence (McKenzie, 1978), yet more studies are revealing the dynamic nature of continental margins, with major post-rift vertical movements further influencing stratigraphic architecture (Morocco – Charton, 2018; Mauritania – Gouiza et al., 2019; French Guiana – Derycke et al. 2018). All these formative processes can invariably lead to a complex structural segmentation of the '*basement*', i.e. crust plus syn- and pre-rift strata, that subsequently controls post-rift depositional systems. Limited studies intrinsically address the margin-scale mega-sequence architecture in the complex geological setting of transform marginal plateaus (TMPs *sensu* Loncke et al., 2020).

The Demerara Rise is a submarine promontory extending from the continental margin over 200 km into the Atlantic Ocean (Fig. 1A), and has an African conjugate, the Guinea Plateau (Jacobi & Hayes, 1982). Both features can be classified as transform marginal plateaus (TMPs) covering a combined surface area of 92,000 km^2 due to the presence of a transform margin (Guinea-Demerara fracture zone) along one flank and the polyphased rifting history. The underlying basement characteristics have been analysed by documenting and interpreting a compilation of basement structures, which are displayed on the top basement structure map (Fig. 1B). This provides a model for the underlying structural framework to assess how basement inheritance may have controlled the structural evolution, subsidence and deposition of the studied overlying post-rift section (Fig. 1B).

Surrounding the Demerara Rise thinned continental crust (Kusznir et al., 2018) and volcanic basement composed of seaward dipping reflectors (SDRs; Reuber et al., 2016), the oceanic crust displays a diachronous accretion due to the dual-phase rifting history. Within the Guyana-Suriname basin the oceanic crust is inferred to be Jurassic in age, whereas to the north and east of the Demerara Rise, in the Equatorial Atlantic domain, oceanic crust is at least 45 Myr younger, accreted during the Upper Cretaceous (Fig. 1; Basile et al., 2005; Reuber et al., 2016). Thus, the dual-phase rifting creates an apparent ocean-ocean boundary northwest of the Demerara Rise where Jurassic and Upper Cretaceous oceanic crust is juxtaposed across the Demerara-Guinea transform. This

ACCEPTED MANUSCRIPT

Downloaded from http://pg.lyellcollection.org/ at University of Manchester, The John Rylands University Library on February 1, 2021

heterogeneity is reflected in the basement morphology of the Demerara Rise, which is more complex than a typical continental margin (i.e. US Atlantic margin – Bally, 1981), rising from subsurface depths below -12,000 m (old Jurassic oceanic crust) to -4,000 m depth along the eastern margin of the Demerara Rise (Fig. 1B).

Investigating how the basement heterogeneity and structural inheritance subsequently controls post-rift sedimentation provides insights to better characterise the highly prospective world-class petroleum systems in the post-rift section, reducing uncertainty and risk for future exploration programmes. Our study integrates geological and geophysical approaches by refining the Mesozoic stratigraphic framework through resampling and analysis of exploration well data, and cores from the Deep Sea Drilling Project (DSDP) and Ocean Drilling Project (ODP) boreholes. This provides a template to constrain the timing of key stratigraphic events during the post-rift history. Results are then extrapolated to a margin-scale seismic reflection dataset to understand lateral (along strike) heterogeneity and segmentation in depositional systems, which we predict were influenced by the dual-phase rifting and underlying structural inheritance.

Regional Setting

The Guyanas continental margin of South America extends 1500 km from the Barbados Prism in the west through the Guyana-Suriname basin and across the Demerara Rise into the Equatorial Atlantic offshore French Guiana, and the Foz do Amazonas basin, Brazil (Fig. 1A). This margin is situated on the north-eastern rim of the Archean Guiana Shield (Fig. 1B). The Demerara Rise, a prominent bathymetric feature, divides the margin into two tectonic domains, the Central Atlantic passive margin to the west, and the Equatorial Atlantic transform margin to the east marking the opening of North America and Africa, and South America and Africa respectively. Consequently, the offshore stratigraphy records the opening of the Central Atlantic (170 Ma; Labails et al., 2010), and Equatorial Atlantic (105 Ma; Sibuet and Mascle, 1978) as the African plate rotated anticlockwise and rifted away from South America. Prior to this later rifting and establishment of the Guinea-Demerara transform, the Demerara Rise formed the southern extension of the Guinea Plateau conjugate margin and hence the key study area for Atlantic plate reconstructions (Pindell, 1985; Moulin et al., 2010; Kneller and Johnson, 2011; Heine et al., 2013). Jurassic post-rift sedimentation on the sutured south-eastern margin of the Central Atlantic initiated with the establishment of an extensive, basin-fringing carbonate platform (Fig. 2; Davison, 2005). The south-eastern extension of the Jurassic-Lower Cretaceous Central Atlantic Ocean formed an arcuate siliciclastic shoreline at the neck of the Equatorial Atlantic across the Demerara Rise (Gouyet et al., 1994).

Opening of the Equatorial Atlantic punctuated this tectonically-quiescent period of Jurassic to Lower Cretaceous passive margin subsidence, which is expressed on the adjacent transform margin and on the West African conjugate as an Aptian unconformity associated with the onset of South Atlantic rifting (Sapin et al., 2016; Olyphant et al., 2017). Barremian-Aptian volcanism linked to Equatorial Atlantic breakup is locally developed on both the Guyanas (Gouyet, 1988; Greenroyd et al., 2008b) and African margin (Olyphant et al., 2017). The Equatorial Atlantic basins developed as a series of en-échelon pull-apart basins separated by paleo-dextral transform faults, now preserved as fracture zones (Pindell, 1985; Greenroyd et al., 2007, 2008a; Basile et al., 2013). Adjacent to this, on the northern margin of the Demerara Rise, compressional structural features are observed below a peneplaned Albian-aged angular unconformity (Gouyet, 1988; Reuber et al., 2016). Transgression

ACCEPTED MANUSCRIPT

Downloaded from http://pg.lyellcollection.org/ at University of Manchester, The John Rylands University Library on February 1, 2021

and opening of the Equatorial Atlantic gateway between the Central and South Atlantic followed (Gasperini et al., 2001; Friedrich and Erbacher, 2006). Cenomanian to Coniacian organic-rich sediments deposited along the Guyanas margin (Canje Formation), and in adjacent basins (i.e. Naparima Hill Formation, Trinidad; La Luna Formation, Venezuela and Colombia). These form prolific hydrocarbon source rocks (Erlich et al., 2003; Meyers et al., 2006). Thermal subsidence of the continental margin and denudation of the Guiana Shield resulted in increased sedimentation rates through the Late Cretaceous (Benkhelil et al., 1995; Yang and Escalona, 2011; Mourlot, 2018). Major uplift of the South American cratons led to the formation of the Purus Arch induced by Andean tectonism during the Paleogene-Miocene (Sapin et al., 2016). This initiated the transcontinental Amazon River, debouching significant volumes of sediment in a depocentre along the margin that persists to present-day (Fig. 1A; Figueiredo et al., 2009).

Previous Studies

The exploration well A2-1 drilled by Esso in 1978 reached total depth (TD) in reported Middle Jurassic-aged (Callovian, 166-163 Ma) sediments (Fig. 1A; Staatsolie, Suriname National Oil Company, 2013), and hence was regarded as the oldest stratigraphic test. Significantly, as part of this study we have re-dated the basal section of this well, determining a late Tithonian age (153-145 Ma) that is younger by at least 10 My. Biostratigraphic detail and implications of the new age dating are provided later in this paper. This key well has been fundamental to the understanding of the stratigraphic evolution of the Guyana margin as the well records the oldest and most-complete post-rift stratigraphy (i.e. Gouyet, 1988; Gouyet et al., 1994; Erbacher et al. 2004a; Kean et al., 2007; Reuber et al., 2016; Griffith, 2017). The Deep Sea Drilling Project (DSDP) collected data from the Cretaceous sequence to investigate the early evolution of the Central Atlantic on Leg 14 at Site 144 (Fig. 1A; Hayes et al., 1972). More recently, the Ocean Drilling Project (ODP) studied the opening of the Equatorial Atlantic Gateway by drilling sites on Leg 207 (Fig. 1A; Erbacher et al., 2004a). This provided the scientific community with core data from the Late Cretaceous to recent sequence, and subsequent studies have significantly improved the existing stratigraphic framework (Erbacher et al., 2004a; 2004b; Erbacher et al., 2005; Mosher et al., 2005; Friedrich and Erbacher, 2006; Hardas and Mutterlose, 2006; Kulhanek and Wise, 2006; Thibault and Gardin, 2006; Krauspenhar et al., 2014). Yang and Escalona (2014) used existing industry data to propose the tectono-stratigraphic evolution of the Guyana-Suriname basin. Post-Albian sedimentary evolution of the Demerara Rise is investigated in Tallobre et al. (2016) and Fanget et al. (2020) focussing on documentation of contourite deposits related to the North Atlantic Deep-Water current. Re-evaluating and integrating these data with our new results along the full extent of the margin strengthens our understanding of the stratigraphic evolution.

Dataset & Methods

Data

Lithological Samples

Re-sampling the DSDP Site 144 and ODP Leg 207 cores took place during 2017-2018, at the IODP Bremen Core Repository, Germany (request ID: 054376IODP, 065859IODP and 077865IODP). Drill

ACCEPTED MANUSCRIPT

Downloaded from http://pg.lyellcollection.org/ at University of Manchester, The John Rylands University Library on February 1, 2021

cutting samples from the exploration wells (A2-1, FG2-1, GM-ES-3) were collected from the CGG Schulenburg facility, Houston, United-States in 2018, kindly donated by Shell. The remainder of these samples are stored for reference in the North Africa Research Group collection at the University of Manchester. A sample summary is provided in the supplementary data (**Error! Reference source not found.**).

Subsurface Seismic and Well Data

The seismic reflection data used in this study offshore northeast South America consists of 34 two-dimensional (2D) seismic reflection profiles (total of 7970 line km) from the ION Geophysical GuyanaSPAN survey (Fig. 1A). The survey images the entire continental margin in water depths of 40-3500 m, with a 50 m shot spacing, recording to 40 km depth and was provided as Pre-Stack Depth Migrated (PSDM) SEGY data. The Suriname – French Guiana ION data is reprocessed data using WiBand broadband technology, recording to 25 km depth. A comparison is made to the conjugate Guinea Plateau. Wireline logs (gamma ray and sonic) for the exploration wells were provided by Shell, and downloaded from the IODP data repository for ODP Leg 207.

Methods

A multi-disciplinary approach has been adopted to investigate and integrate a large subsurface dataset with existing studies to document continental margin evolution.

Sedimentology and Organic Geochemistry

Drill cutting samples were set in resin and thin sectioned for petrographic analysis using an optical light microscope. Descriptive petrographic sandstone classification was performed after Garzanti (2016). Whole-rock X-Ray diffraction (XRD) was performed at BGS Keyworth on samples from FG2-1 using PANalytical X'Pert Pro series diffractometer and the quantification methods of Snyder and Bish (1989).

Sixty-five shale samples were selected for organic geochemical analysis using a Shimadzu TOC-V CPN and Solid Sample Module (SSM), calibrated to sodium carbonate and glucose to measure inorganic and total carbon respectively. Additional geochemical data for ODP Site 1258C was incorporated from Meyers et al. (2006). TOC data generated from the analysis of cuttings (exploration wells) is expected to yield lower results due to the contaminant and mixing with other lithologies, as compared to core data (DSDP Site 144).

Further geochemical characterisation of thirty-four samples yielding greater than 0.5% TOC was completed using a Rock-Eval 6 instrument at the University of Greenwich. Measurements of TOC are consistently less than TOC derived from the Rock-Eval, by on average 0.53%. We report the results from the separate TOC analysis as this is often a more reliable measurement of TOC compared to results from the Rock-Eval 6 (see Behar et al., 2001). Additionally, a solvent was not used to remove free hydrocarbons prior to the pyrolysis, whereas in the TOC analysis, free hydrocarbons are generally removed during the process, leading to a higher value from the Rock-Eval.

ACCEPTED MANUSCRIPT

Downloaded from http://pg.lyellcollection.org/ at University of Manchester, The John Rylands University Library on February 1, 2021

Four samples from well A2-1 at Aptian and older levels with reported hydrocarbon shows were sent to GeoMark Research, Houston for hydrocarbon extract analysis. Extracts were analysed for high resolution gas chromatography and biomarker geochemical analysis.

Biostratigraphy

Dependent on lithology, various biostratigraphic analyses were performed to provide age constraints on the stratigraphy. All key biostratigraphic events are shown on Fig. 2 and Table S1 is provided to highlight which samples were analysed using the different techniques. *Calcareous nannofossils* (Jason Jeremiah): In total 138 samples (see Table S2 for the nannofossil event charts by well) were analysed with standard techniques described by Bown (1998), and the picking brush method of Jeremiah (1996). Samples were analysed semi-quantitatively, with the first thirty fields of view counted and the remaining slide scanned for rare specimens. Specimens are photographed in Fig. S2 and further text describing the taxonomy of new specimens is provided in the supplementary data. *Foraminifera* (Mike Bidgood): Thirty-one samples with relatively abundant calcareous nannofossil content were chosen for micropaleontological analysis and prepared using the standard methodology described by Armstrong and Brasier (2013). *Palynology* (Frédéric de Ville de Goyet): Ten samples for palynological analyses were subject to the standard palynological preparation technique which involves removal of all mineral material by hydrofluoric acid digestion and sieving to produce a residue of the 10 micron and above size fraction for each sample. An initial count of 100 in situ palynomorph specimens was performed and abundance quantitatively assessed using percentage of total palynoflora. The palynology charts are provided in Fig. S3. *Calpionellids* (Daniela Reháková): A total of eight limestone-rich cutting samples from well A2-1 were thin sectioned and petrographically analysed for the occurrence of calpionellids. Results are amalgamated within the '*dating*' section of each well/borehole, therefore the letters (N), (F), (P) and (C) are used to denote the type of fauna, calcareous nannofossils, foraminifera, palynology, calpionellids respectively, when discussed.

Cuttings samples are (theoretically) composited, representative material from a drilled interval of rock. Cuttings are susceptible to contamination from material collapsing into the borehole (called "cavings") from levels higher in the section and contaminating *in situ* sample material from near the drill bit. To mitigate contamination from cavings, multiple picked lithologies per sample were analysed for nannofossils, the oldest sample being considered representative of the depth, first occurrence (FO's) and last occurrence datums (LO's) were then utilised. This was not possible for the palynology and foraminiferal work where more rock material is required, extinction events (or events which become apparent in a downhole perspective) form the basis for the majority of biostratigraphic determinations i.e. first downhole occurrence, FDO.

Seismic Interpretation & Structural Evolution

To ensure a robust seismic-well tie and depth calibration, synthetic seismograms for two exploration wells, A2-1 and FG2-1, plus the ODP Leg 207 boreholes were produced. This process tied the wireline log data to the seismic survey following the methodology of Sheriff (1976; 1977). Despiked sonic logs were converted to give an estimation of the density log using Gardner's equation. Statistical wavelets were extracted for A2-1 and FG2-1 from the zones of interest, 2000 – 4000 m and 2000 – 3500 m depth respectively (Fig. 10). Following this, key horizons (Fig. 2) identified during the

ACCEPTED MANUSCRIPT

Downloaded from http://pg.lyellcollection.org/ at University of Manchester, The John Rylands University Library on February 1, 2021

stratigraphic re-evaluation were interpreted on the 2D seismic dataset using Schlumberger's Petrel software and the interpretation methods of Payton (1977). Horizons were gridded and isochore thickness maps calculated for three gross megasequences (Fig. 12). Flattening of the seismic section (Fig. 11A) on key horizons helped improve our understanding of depositional geometries and structural features at the time of deposition (Fig. 14; Bland et al., 2004). Projecting the uppermost continuous seismic reflector below the base Albian unconformity (BAU) provided an estimation for the amount of missing section due to erosion.

Results

Sedimentological & Stratigraphic Control

Seven wells and scientific boreholes in the study area provide the control on lithologies/facies, age dating and organic geochemistry. These have been re-examined and the new data used to build depositional models to constrain and be integrated into the seismic dataset. Sample depths are reported in the original unit of measurement, a metric conversion is provided for imperial depth measurements.

GM-ES-3

Exploratory drilling offshore French Guiana targeted the Santonian to Maastrichtian-aged Cingulata turbidite fan system (McCoss, 2017). Through 2011-2013, 5 exploration wells were drilled with the first, GM-ES-1 (Zaedyus), encountering 72 m of net oil pay. Subsequent wells failed to find commercial hydrocarbons in adjacent prospects due to failure of the stratigraphic traps. This includes GM-ES-3 (Priodontes), which penetrated a 50 m gross section of oil-stained sandstone reservoir (Bradypus fan) above the targeted water-wet reservoir (Priodontes fan), well failure as a result of an invalid trap. The 670 m thick sequence below the reservoir section to TD is mudstone-dominated with calcareous and organic-rich intervals. At 6036 m, there is a lithology change from shale to non-calcareous mudstones and at TD, sandstones, considered to be pre-rift strata. The data from this well provides crucial stratigraphic information of deposits recording the rift-to-drift transition and timing of breakup in the Equatorial Atlantic (Fig. 3).

Dating – The current study investigates the pre-Coniacian/Santonian reservoir section in GM-ES-3 (Fig. 3), all the age dating is based on calcareous nannofossils (N). The interval 5760 m – 5830 m confirms a complete Turonian sequence. Penetration of the latest Turonian is confirmed at 5760m with the presence of an influx *Marthasterites furcatus* below the FO of *Micula staurophora*. An age no older than Middle Turonian is confirmed with the FO of *Eiffellithus eximius* at 5780m. Earliest Turonian sediments characterised by the quantitative influx of *Eprolithus moratus* and *E. floralis* occur between 5800 m – 5830 m, events below the FO of *Quadrum gartneri* at 5780 m. The OAE-2 interval is postulated at approximately 5820 m where there is a subtle peak in the gamma ray log, likely subdued in comparison to other studied wells due to turbidite input nearby (encountered in GM-ES-1). This occurs within Early Turonian aged sediments, typically latest Cenomanian with the top at the Cenomanian-Turonian boundary, we postulate this is either due to log to drillers discrepancy or just rarity of top Cenomanian markers at this point. Penetration of Cenomanian-aged strata is proven by the LO of *Axopodorhabdus albianus* at 5850 m. Middle – Lower Cenomanian strata occur at 5940 m with the LO's of *Gartnerago nanum* and *G. theta*. The LO of consistent

ACCEPTED MANUSCRIPT

Downloaded from http://pg.lyellcollection.org/ at University of Manchester, The John Rylands University Library on February 1, 2021

Eiffellithus paragogus at 6000 m confirms penetration of the Lower Cenomanian (Burnett, 1998; Ando et. al., 2015; Chin 2016), Cenomanian sediments are proven as deep as 6020 m – 6040 m with the occurrence of *Corollithion kennedyi* and FO's of common *Broinsonia signata*.

Upper Albian is confirmed at 6060 m, with the consistent LO of *Braarudosphaera* spp. including *B. stenorhetha.* The excellent preservation is reflected in the preservation of *B. primula dodecahedra*. A marked decrease in braarudosphaeres was recorded towards top Albian from ODP Leg 171B, Site 1052E off the Blake Nose plateau by Watkins et al. (2005), a similar top to a *Braarudosphaera quinquecostata* acme event from Texas and Oklahoma by Hill (1976) and downhole increase in *B. primula* often associated with *B. stenorhetha* from the offshore Gulf of Mexico (pers. obs.), and offshore Morocco (Chin, 2016). Although *Nannoconus* spp. including *N. quadriangulus quadriangulus* and *N. q. apertus* are consistently observed the Late Albian quantitative acme recorded by Watkins et al., (2005) and Hill (1976) is not recorded from offshore Suriname.

GM-ES-3 is unusual in the current study in having a relatively expanded latest Albian section (NC10a upper) between 6060 m – 6130 m. At 6140 m, the LO of *Eiffellithus monechiae* is recorded, its co-occurrence with equal numbers of *Eiffellithus turriseiffelii* down to 6170 m proving an age no older than the lower part of NC10 (Jeremiah, 1996; Bown, 2001; Gale et. al., 2011a). Marine Late Albian mudstones rest directly upon non-marine rift sandstones at TD (palynology results; Shell).

French Guiana 2-1 (FG2-1)

Well FG2-1 was spud in 1978 by ESSO, the main objective being Lower Cretaceous clastics and underlying carbonates in a structural closure. The well was dry, probably drilled off structure in a hydrocarbon fairway shadow, Late Cretaceous source rocks penetrated at the well were immature. Well FG2-1 is unique along the continental margin as it reaches TD in a 380 m thick succession of basalts previously reported as 125 Ma in age (Barremian; Fig. 1B; Gouyet et al., 1994), 120 ± 6 Ma (ESSO, 1978). Whole rock XRD shows the volcanics to have a mafic composition, predominantly plagioclase and pyroxene with smectite, chlorite, quartz and magnetite. Smectite likely originates from weathered basalts. 50 m of oxidised red sands overlie this unit, suggesting subaerial exposure (Fig. 4). About 470 m of very-fine to fine grained litho-quartzose sandstone with clay matrix is encountered above this. Petrographical investigation reveals the sands are poorly sorted and matrix supported, with sub-angular quartz grains and additional lithic clasts of reworked sedimentary material (**Error! Reference source not found.**). These sands were likely deposited in a non-marine/continental environment as no marine fauna or glauconite were observed in the petrographical analysis. At 3030 m depth, there is a lithological break recorded as a positive shift in the gamma ray log, sediments above this surface are calcareous organic-rich mudstones recording the first marine influenced strata.

Dating – Nannofossil and foraminifera analysis started at 7600 ft (2316.50 m) within lower Thanetian sediments, based on the co-occurrence of *Heliolithus kleinpellii*, *Discoaster mohleri* (N) and FDO of *Globanomalina pseudomenardii* (F). This level is just above the Base Tertiary unconformity (BTU) identified at 2329.79 m. Lower Paleocene and Upper Maastrichtian deposits appear missing, this sequence is not encountered in subsequent cavings. A diverse Lower Maastrichtian assemblage is recovered from the interval 7800 ft – 8000 ft (2377.4 m – 2438.4 m) with *Reinhardtites levis* (N) recorded, supported by the FDO of *Globotruncana aegyptiaca* (F). At 8200 ft (2499.4 m) the LO's of

ACCEPTED MANUSCRIPT

Downloaded from http://pg.lyellcollection.org/ at University of Manchester, The John Rylands University Library on February 1, 2021

Marthasterites furcatus, common *Eiffellithus eximius*, *Lithastrinus grillii* and *Broinsonia signata* (N) indicates basal Campanian deposits.

A relatively complete Santonian to Coniacian sequence is penetrated between 8400 ft – 8980 ft (2560.3 m – 2737.1 m). At 8400 ft (2560.3 m) Lower Santonian deposits are proven with the LO of *Lithastrinus septenarius* (N). The LO of *Quadrum gartneri* and *Q. eneabrachium* (N) is at 8780 ft (2676.1 m) followed by the FO of *Micula staurophora* and LO of *Eprolithus floralis* (N) at 8980 ft (2737.1 m). This is supported by the foraminifera analysis where the FDO of *Marginotrucana sigmoconcavata* (F) indicates an age no younger than Santonian (intra-*Dicarinella asymetrica* zone) at 8400 ft (2560.3 m). The presence of common *Marginotruncana* spp. (F) in assemblages at and below this depth support the age assignment. This genus is restricted to the Santonian – Turonian interval.

Turonian sediments are recorded from 9200 ft (2804.2 m), this interval below the FO of *Micula staurophora* (N) and supported by the FDO of *Praeglobotruncana* spp. (F). The base of the Middle Turonian is marked by both FO's of *Marthasterites furcatus* and *Eiffellithus eximius* (N) at 9400 ft (2865.1 m). The Upper Cenomanian is penetrated at 9790 ft (2984.0 m) characterised by the LO of *Axopodorhabdus albianus* and *Gartnerago praeobliquum* (N). Between 9820 ft (2993.1 m) and 9890 ft (3014.5 m) the cuttings are dominated by Upper Turonian cavings, no *in-situ* assemblages are recovered. Penetration of Middle to Lower Cenomanian is confirmed by the LO's of *Gartnerago theta* and *G. nanum* (N) at 9920 ft (3023.6 m). The oldest sample from 9950 ft (3032.5 m) yields *Corollithion kennedyi*, abundant *Broinsonia enormis* and *G. nanum* (N) confirming Cenomanian sediments, Upper Albian deposits absent.

Three samples from the sandstones overlying the volcanics were analysed for palynology (3072.4 to 3288.8 m; Fig. 4), however, the samples were dominated by Late Cenomanian cavings.

Demerara A2-1

A2-1 was spudded by Esso in 1977 in 3937 ft (1200 m) water depth to appraise a large anticlinal structure over the Demerara Rise, offshore Suriname. The well was drilled to a total measured depth of 16207 ft (4940.0 m) within previously reported Middle Jurassic (Callovian) platform carbonates and abandoned as a dry well, likely failing due to a lack of hydrocarbon charge. The lowermost *ca*. 2350 m of stratigraphy in A2-1 is composed mainly of an alternating limestone/mudstone sequence (Fig. 5). Limestone-dominated strata sharply decrease the gamma ray log forming distinctive blocky responses (Fig. 5; Fig. 10), these sequences are up to 450 m thick. Petrographic analysis of these limestones reveals a mixture of microfacies within the cuttings; biomicritic, bioclastic, sandy, silty limestones are observed with a mudstone to grainstone texture, occasionally dolomitised. Limestones rich in bioclastic material contain fragments of ostracods, crinoids, spores, echinoid spines, recrystalised bivalve shells, framboidal pyrite, representative of platform carbonates. The micro-fauna includes planktonic foraminifera observed in most limestone cuttings, with common cysts and spores, and occasional calpionellids (discussed below). Two samples from near TD of the well contain more argillaceous and siliciclastic material with minor organic matter. Sedimentation rates are relatively high averaging 65.8 m/Myr throughout this interval (Fig. 2). This sequence is more mudstone-dominated towards the top, becoming increasingly organic (max. TOC – 1.09%).

ACCEPTED MANUSCRIPT

Downloaded from http://pg.lyellcollection.org/ at University of Manchester, The John Rylands University Library on February 1, 2021

A 40 m thick sandstone unit with remarkably similar lithological characteristics to the fine-grained sands in FG2-1 overlies this package and is interpreted as part of the Starbroek Formation (**Error! Reference source not found.**). Of note, the presence of glauconite is indicative of deposition in shallow marine conditions (e.g. Stonecipher, 1999; **Error! Reference source not found.**) and sedimentation rates. Limestones (Potoco Formation), 80 m thick, overlie these sands and are the first transgressive deposits above the BAU. The overlying unit is marked by a sharp increase in the gamma ray log. A thick interval of calcareous mudstone is encountered with high organic content and is eventually truncated by the BTU.

Dating – The youngest samples analysed at 7020 ft (2139.7 m) yielded a middle Campanian assemblage characterised by *Eiffelithus eximius*, *Uniplanarius sissinghi* and *Arkhangelskiellla cymbiformis* (N), and FDOs of *Contusotruncana fornicata*, *C. ?contusa* and *Rugotruncana subcircumnodifer* (F). The middle Campanian unconformity (MCU) is recognised in this well at 2156.65 m, with the underlying sediments recorded from 7110 ft (2167.1 m) yielding Santonian fauna characterised by *Marthasterites furcatus, Lithastrinus grillii* (N) below FO's of the *Broinsonia parca* group and *A. cymbiformis* (N). Organic mudstones of Coniacian to ?Upper Turonian age are recovered over the interval 7260 ft – 7290 ft (2212.8 m – 2222.0 m). The assemblages are characterised by *Quadrum gartneri, Eprolithus floralis* and *Lithastrinus septenarius* (N). The FO of *Micula staurophora* (N) at 7290 ft (2212.8 m; if *in-situ*) would indicate an age no older than Coniacian. The occurrence of abundant *M. furcatus* (N) also at 7290 ft (2212.8 m) confirms an age no older than uppermost Turonian.

A relatively expanded Lower Turonian succession between 7410 ft – 7650 ft (2258.6 m – 2331.7 m) is characterised by the HRA of *Eprolithus* spp. (N) including quantitative influxes of *Eprolithus moratus* and *E. floralis* (N) below the FO of *Eiffelithus eximius* (N). The LO of *Zeugrhabdotus scutula* ssp. *turonicus* (N) is at 7500 ft (2286.0 m), whilst the FO of *Quadrum gartneri* (N) is at 7590 ft (2313.4 m). The age assignment is supported by FDOs of *Whiteinella aprica* and ?*W. inornata* (F). Penetration of Upper Cenomanian strata is confirmed by the LO's of *Axopodorhabdus albianus, Gartnerago praeobliquum* and *Helenea chiastia* co-occurring with *Gartnerago obliquum* (N) at 7710 ft (2350.0 m). Lower Cenomanian age is penetrated at 7800 ft (2377.4 m) with the LO's of *Gartnerago nanum* and *G. theta* (N), the age assignment supported by the LO of consistent *Eiffellithus paragogus* at 7840ft (2389.63m). The basal Cenomanian is characterised by the *Broinsonia plexus* including *B. cenomanicus*, *B. signata* and *B. enormis* (N). Other characteristic nannofloral events of the basal Cenomanian is the HRA of *Helicolithus compactus*, *H. compactus* (small var.) and *Gartnerago praeobliquum* (small var.). At well A2-1 the base Cenomanian unconformity lies directly upon a ?Lower Albian Potoco carbonate succession, no Upper to Middle Albian preserved as at ODP Leg 207 (Erbacher et al., 2004a).

The mudstone-dominated sequence below the BAU at 2496.4 m yields an intra-early Aptian to ?Barremian marine dinocyst assemblage due to the presence of *Pseudoceratium pelliferum* (Duxbury, 1983), *Achomosphaera verdierii* (Below, 1982) and *Afropollis zonatus* (Doyle et al., 1982; P). The co-occurrence of common *Dicheiropollis etruscus*, is a sporomorph event which has been recorded from unpublished data of Atlantic offshore Morocco within Hauterivian dated sediments. It is widely recorded from undifferentiated Neocomian sediments offshore West Africa) and *Muderongia simplex microperforata* (Davey, 1982; Costa et al., 1992; P).

ACCEPTED MANUSCRIPT

Downloaded from http://pg.lyellcollection.org/ at University of Manchester, The John Rylands University Library on February 1, 2021

Between 10840 ft (3307.1 m) and 11790 ft (3593.6 m) rich nannofloras yielding *Eiffellithus windii, E. striatus, Stradnerlithus silvaradius, Rhagodiscus dekaenelii, R. manifestus, Speetonia colligata, Cruciellipsis cuvillieri,* abundant *Cyclagelosphaera margerelii, C. brezae, Tubodiscus verenae* and *Tripinnalithus surinamensis* (N) are encountered indicating penetration of late Valanginian sediments. Sporadic occurrences of *Calcicalathina oblongata* and *Diadorhombus rectus* (N) are also recorded. Nannoconids are dominated by the wide canal species *N. kamptneri*, *N. wassalii* and *N. cornuta* (N). The late Valanginian appears to record the Lower Cretaceous maximum sea level pre-Albian and associated increase in nannofloral diversity. This level is calibrated to the Upper Valanginian MFS (VF), an event recorded in this study from the Gulf of Mexico (Loucks et al., 2017; Jeremiah, pers. obs.).

Below 11790 ft (3593.6 m), nannofossil diversity decreases with the increased frequency of platform limestones. A brief flooding event is recorded between 12850 ft (3916.7 m) and 13090 ft (3989.8 m), where calcareous mudstones are encountered again. The nannoflora is characterised by *Crucibiscutum salebrosum, Nannoconus steinmannii minor*, *Diadorhombus rectus*, *Eiffellithus primus and Tubodiscus verenae* below the FO of *Calcicalithina oblongata* (N), an indication that late Berriasian sediments have been penetrated.

The current biostratigraphy study confirms the age at TD of this well as no older than late Tithonian based on calpionellid occurrences, much younger than previous studies that indicate an age as old as Callovian (Griffith, 2017). The majority of the carbonate succession is Early Cretaceous aged. At 14100 ft (4297.7 m) the top occurrence of *Crassicollaria intermedia* (C) is recorded, indicating the late Tithonian has been penetrated, specifically the *Crassicollaria* Zone (Rename, 1985; Blau & Grün, 1997). Below this, the top occurrence of *Calpionella alpina* and *Crassicollaria parvula* (C) occur at 15100 ft (4602.5 m), as well as occurrences of *Calpionella alpina, Crassicollaria intermedia* and *Tintinnopsella carpathica* (C) at 15590 ft (4751.8 m) are again characteristic of the late Tithonian *Crassicollaria* Zone. The acme of *Calpionella alpina,* diagnostic of the Jurassic-Cretaceous boundary (Michalík & Reháková, 2011; Wimbledon et al., 2011), is not recorded likely due to the studied sampling interval and therefore a tentative top Jurassic is placed at 4277.1 m. Three samples from the interval 15330 ft – 16070 ft (4672.6 m – 4898.1 m) yield a low diversity dinocyst assemblage of *Amphorula metaelliptica* (Dodekova, 1969; Monteil, 1992; Habib & Drugg, 1983; van Helden, 1986), *Oligosphaeridium diluculum* (Davey, 1982) and *Pseudoceratium pelliferum* (P), indicating an age no older than Berriasian, the assemblage considered caved.

ODP Leg 207

The following lithological summary is provided for the Cretaceous sediments of Site 1258C (the main focus of the study), however a more complete description of the stratigraphy penetrated on Leg 207 and specifically Site 1258 is presented in Erbacher et al. (2004a; 2004b; Fig. 6). Additional data is presented from sites 1257A and 1260A. Cores from three Cretaceous units were recovered (Fig. 7): Unit 3 – calcareous nannofossil clay (139 m); Unit 4 – laminated black shale and limestone (55 m); Unit 5 – phosphoritic calcareous clay with organic matter (thickness – 37 m). The top of Unit 3 is marked by 2 cm thick layer of graded medium to fine-sized green spherules representing the ejecta layer of the Cretaceous-Tertiary (K/T) boundary (Erbacher et al., 2004a; 2004b). The uppermost section of Unit 5, Core 27 (Fig. 7) is calcified and indurated interpreted to be indicative of multiple unconformities, hiatus and condensation, supported by low sedimentation rates (<5 m / Myr; Fig. 2).

ACCEPTED MANUSCRIPT

Downloaded from http://pg.lyellcollection.org/ at University of Manchester, The John Rylands University Library on February 1, 2021

Dating – All dates have been determined from calcareous nannofossil analysis (N). At Site 1258C, Erbacher et al. (2004b) described a Campanian unconformity, with the early Campanian to Santonian absent. This MCU is confirmed at the base of Core 15 -3 (Fig. 7), middle Campanian chalks yielding *Eiffelithus eximius*, *Broinsonia enormis, Broinsonia parca constricta* and *Arkhangelskilella cymbiformis* immediately above a condensed Middle Turonian organic shale succession with *Quadrum gartneri* and *Lithastrinus septenarius* recorded at 393.77 m. Erbacher et al. (2004a) documented younger Coniacian organic mudstones preserved beneath the unconformity south-eastwards at Site 1260. This is supported by sediments as young as Santonian age preserved beneath the MCU at well A2-1 (Fig. 5).

Hardas and Mutterlose (2006) investigated the Cenomanian-Turonian boundary from Site 1258C and recorded the LO of the Cenomanian marker, *Axopodorhabdus albianus* at 400.55 m. Due to a sample gap, penetration of Cenomanian strata is confirmed slightly lower in the current study at 404.30 m, the LO's of *Axopodorhabdus albianus* and *Gartnerago praeobliquum* recorded.

Lower Cenomanian sediments are proven at 428.95m with the occurrence of common *Gartnerago theta,* the age assignment supported by the LO of consistent *Eiffellithus paragogus* at 438.32m. Cenomanian strata are confirmed down to 447.58 m at Site 1258C with the FO of *Corollithion kennedyi*. Erbacher et al. (2004b) documented a major hiatus at the base Cenomanian with no support for the preservation of Upper Albian sediments. The current study supports the identification of the base Cenomanian unconformity, with latest Albian sediments missing. The upper part of Zone NC10 is not recorded. Intra Late Albian aged sediment is however recorded immediately below at 449.74m with the LO of an increase in *Eiffellithus monechiae*, *E. turriseiffelii*, however still quantitatively dominant over *E. monechiae*, down to 450.06m.

The FO of *E. turriseiffelii* and associated *E. monechiae* acme and earlier FO is not preserved in 1258C. Another hiatus, an intra Late Albian unconformity is recorded from the base of Core 27-2 at 450.16m, sediments occurring below characterised by *Staurolithites angustus* at 450.45m. The LO's of *Watznaueria britannica* and *Hayesites albiensis* are both recorded from 450.45m, these forms utilised as alternative top Albian markers (Watkins and Bowdler, 1984; Burnett, 1998); their occurrences here depressed stratigraphically but of potential local correlative significance. Another major change in nannoflora at this stratigraphical level is the increase downhole of cold-water nannofossils such as the HRA of *Repagulum parvidentatum* below 450.45 m and consistent *Seribiscutum primitivum* below 451.85 m, events also recorded by Kulhanek and Wise (2006).

The oldest definitive Late Albian sediments at Site 1258C are confirmed by the FO of *Staurolithites angustus* and consistent *Cribrosphaerella ehrenbergii* (Jeremiah, 1996; 2001; Bown, 2001) at 456.84 m (Core 29-1). Additionally, an assemblage of ammonites collected and examined by Owen and Mutterlose (2006) from cores 30 and 31, Site 1258C refine this age assignment to early Late Albian within the *Hysteroceras varicosum* Zone. Late Albian sediments are potentially confirmed as deep as 467.94 m with the FO of *Crucibiscutum hayi* (Jeremiah, 1996; Bown, 2001; Gale et. al., 2011); similar forms though are known to range down into the Middle Albian (Jeremiah, 1996). Hence in the current paper are assigned the ranged Middle-Late Albian age.

Kulhanek and Wise (2006) also recorded *Eiffelithus monechiae* consistently down to Core 33-2, *Cribrosphaerella eherenbergii* almost to the base of the cored section at Core 34-2 and the boreal Upper Albian marker *Tegulalithus tessellatus* between Cores 33-2 and 34-2. All these markers are

ACCEPTED MANUSCRIPT

Downloaded from http://pg.lyellcollection.org/ at University of Manchester, The John Rylands University Library on February 1, 2021

Upper Albian restricted but could not be corroborated in the current study at these deeper levels within the core. The interval 459.85 m – 484.82 m yields an early Late Albian through late Middle Albian nannoflora. Boreal markers that would enable further subdivision of the early Late Albian through Middle Albian succession such as *Tegulalithus tessellatus*, the *Ceratolithina plexus* and *Braloweria boletiformis* are all absent. The consistent occurrence of *Axopodorhabdus albianus* to the base of the cored section at 484.82 m, however, confirms an age no older than late Middle Albian.

Sporadic records of *Axopodorhabdus albianus* are recorded from the lower Middle Albian (Jeremiah, 1996, 2001; Bown, 2001; this study DSDP144; 299.28 m). Base consistent *A. albianus* from the upper Middle Albian was preferred by Jeremiah (1996, 2001; Bown, 2001) as a cosmopolitan event and supported by observations from Texas by Hill (1976) and Bralower et al., 1993.

The oldest cored sediments investigated from the Demerara Rise on ODP Leg 207 were found at sites 1257A and 1260A. Here, early Middle Albian nannofloral assemblages were recovered similar to that recorded from DSDP Leg 14, Site 144 (**Error! Reference source not found.**).

DSDP Leg 14 Site 144

The objective of DSDP Leg 14 Site 144 was to recover the oldest marine sediments of the proto-Atlantic (Hayes et al., 1972). Three boreholes (A, B, Z) were drilled to a TD of 327 m recovering 10 cores, totalling 31.9 m in length, from four Cretaceous-aged units (Fig. 8): Unit 2 – zeolitic greenish-grey marl; Unit 3 – black and olive zeolitic marl; Unit 4 – olive green marl; Unit 5 – silty quartzose marl with shelly limestones and background organics. These units differ from the lithostratigraphic units of ODP Leg 207 (Fig. 6; Fig. 7).

Dating – All the age datings are determined from calcareous nannofossil analysis (N). The hiatus associated with the MCU is also recorded at DSDP 144 where late Campanian sediments from the base of Core 4-2 (173.96 m) are recorded only 7 m above Upper to -Middle Turonian sediments at the top of Core 5-1 (Fig. 8). The sample at 181.05 m yields *Eiffellithus eximius* and *Quadrum gartneri* below the FO of *Micula staurophora*. Upper Cenomanian-aged sediments yielding *Gartnerago obliquum*, *G. praeobliquum* and *Axopodorhabdus albianus* are recorded from Cores 4-2 to 4-3 (Fig. 8), equivalent to Core 19-1 at ODP Site 1258C (Fig. 6). An early Middle Albian succession is preserved in the interval 264.14 m – 328.35 m (TD). The base Middle Albian age assignment is supported by the FO of *Tranolithus phacelosus* at 264.14m and absence of consistent *Axopodorhabdus albianus*. A Middle Albian age to the base of the cored section is supported by the presence of *Crucicribrum anglicum* down to 328.35 m. *Braarudosphaera* spp. are recovered including *B. stenorhetha* in association with nannoconids including *Nannoconus quadriangulus quadriangulus* and *N. q. apertus*.

Organic Geochemistry

Combined with re-dating of sediments from the seven wells and scientific boreholes studied, further organic geochemical analysis was undertaken to improve characterisation of the prolific Upper Cretaceous organic-rich interval (Canje Formation) encountered along the continental margin. This source rock in the basin kitchens either side of the Demerara Rise (Fig. 1A) has been generating hydrocarbons from Late Miocene to present-day (James et al., 2020). Hydrocarbons charge turbidite reservoirs in the base-of-slope to basin floor setting in the Guyana-Suriname basin (Cedeño et al., 2019) and offshore French Guiana observed in the GM-ES-1 well, and through long-distance

ACCEPTED MANUSCRIPT

Downloaded from http://pg.lyellcollection.org/ at University of Manchester, The John Rylands University Library on February 1, 2021

migration to the onshore Tambaredjo heavy oil field, Suriname (Fig. 1A; Dronkert & Wong, 1993). Additionally, the new dataset improves our understanding of older source potential (i.e. Jurassic).

The new data generated from DSDP Site 144 and ODP Site 1258C refines the onset of organic-rich sedimentation on the Demerara Rise to occur during the late Middle Albian. Early Middle Albian olive green marls from DSDP Site 144 (and ODP Sites 1257A and 1260A) are organic-lean, with average TOC from cores 5 to 8 at 0.65% (Fig. 8). Whereas, late Middle Albian black shales recovered from ODP Site 1258C average 4.23% TOC (Fig. 6; Fig. 7). Pyrolysis reveals the organic matter is Type II algal material (Unit 4) and mixed Type II/III (Unit 5; Erbacher et al., 2004b).

Throughout the wells, TOC values peak around the Cenomanian-Turonian boundary (~OAE-2), reaching a maximum value at ODP Site 1258C of 28.13% TOC, as recorded globally (Schlanger et al., 1987). This peak is observed in additional exploration wells on the Guyana shelf (AR-1, ESS-2; Fig. 15; Mourlot, 2018), and is commonly associated with a significant peak in the gamma ray log (Fig. 4; Fig. 5). This peak is subdued in GM-ES-3 (Fig. 3), likely due to the proximity of sand dominated turbidite systems suppressing the signature (Fig. 16). In all the wells studied on the Demerara Rise, the Upper Cretaceous organic-rich interval is truncated by the MCU. Campanian organic content is present in FG2-1, documented to be terrestrially-derived (Fig. 9). Average TOC values for the Canje Formation vary along the margin; on the Demerara Rise the highest average TOC values are recorded on the north-western distal margin at DSDP Site 144 (7.22%) and ODP Site 1258C (7.67%). The TOC decreases towards the paleo-coastline in A2-1 to 3.96%, and again at FG2-1 to 2.09% (Fig. 16). In the Equatorial Atlantic domain at GM-ES-3 TOC averages 4.28%.

Source rock maturity indicated by Tmax values range from 346 to 430 °C, averaging 418 °C indicating all samples are immature (**Error! Reference source not found.**). To compare source rock quality and kerogen type, hydrogen and oxygen indices were plotted on a modified van Krevelen diagram (Fig. 9). Raw data is presented in **Error! Reference source not found.**. To understand temporal changes in kerogen type the symbology reflects the age of the sample. The majority of samples have high hydrogen index (HI; 475 to 600+ mg hydrocarbons/g organic carbon) and low oxygen index (OI; 20 to 65 mg CO_2/g organic carbon) indicating Type II marine kerogen with oil generating potential. Outliers from this group with low HI and high OI values are all early Middle Albian in age from DSDP Site 144 (cores 5 to 8) indicative of gas-prone Type III terrestrial kerogen. Younger Albian samples show a progressive increase in HI and decrease in OI towards the Type II group, indicating the gradual increase in marine-type organic matter through this interval. Cenomanian to Coniacian samples from FG2-1 have lower HI and higher OI values (average HI – 251 mg hydrocarbons/g organic carbon; average OI – 76 mg CO_2/g organic carbon) showing a mixing between Type II/III. This reflects the relative position of FG2-1 closer to the paleo-shoreline and sediment input from river systems (Fig. 16) and therefore likely receiving more terrestrial input as indicated by the higher sedimentation rates compared to the time-equivalent interval in A2-1 (Fig. 2). Pyrolysis results from GM-ES-3 fall within a tight grouping away from main Type II signature with low OI (20 to 30 mg CO_2/g organic carbon) and moderate HI (200 to 450 mg hydrocarbons/g organic carbon) values, suggesting a mixing of kerogen types. S_1 peaks are representative of hydrocarbons generated at low temperatures during the pyrolysis and indicate free or absorbed hydrocarbons (Allen & Allen, 2013). Average S_1 values for GM-ES-3 samples are 21.4 mg/g, compared to an average of 1.0 mg/g for all remaining samples, indicating free hydrocarbons throughout the interval analysed in GM-ES-3. Alongside the low Tmax values (immature), this suggests the free hydrocarbons are migratory.

ACCEPTED MANUSCRIPT

Downloaded from http://pg.lyellcollection.org/ at University of Manchester, The John Rylands University Library on February 1, 2021

Geochemical analysis of samples below the BAU in A2-1, i.e. Aptian to Berriasian, all yield low TOC values (average 0.37%). Higher values 1.1 to 1.5% TOC were previously reported by Griffith (2017) from this interval as indicative of a Middle Jurassic (Callovian) syn-rift source rock based on the original biostratigraphy. Our new age dating proves no Callovian sediments were encountered in A2-1, meaning the well did not penetrate a syn-rift source rock below the Demerara Rise. However, this new evidence does not rule out the potential for a Jurassic source rock along the margin. Seismic evidence from this study supports the interpretation of additional older Jurassic sediments below the well TD of A2-1 (Fig. 11), distributed deeper across the Demerara Rise (see Margin Architecture, Fig. 12A – MS1), and onto the Guinea Plateau (Fig. 16A). Oil and gas shows within the Lower Cretaceous interval are reported suggesting deeper source rock potential as the main organic-rich interval sits above the BAU (Fig. 5). Additional support for a potential Jurassic source rock is evidenced by proven Jurassic-aged lacustrine shales with 2.5% TOC within the Takutu Graben onshore (Webster, 2004), and predicted in two grabens (Nickerie, Commeqijine; Fig. 1B) offshore from gravity data (Griffith, 2017). Further geochemical work by Cedeño et al. (2019) of oil recovered from wells onshore Suriname (Tambaredjo field) revealed two hydrocarbon groups, one typed to the proven Upper Cretaceous source rock and another group from a source that generated hydrocarbons from terrestrial organic matter in marly sediments interpreted as Jurassic or Lower Cretaceous in age. These hydrocarbons are postulated to be generated from the Lower Cretaceous interval penetrated by A2-1.

The hydrocarbons at the Liza and Tambaredjo fields have migrated out of the deep Guyana-Suriname basin from the Canje Formation, sitting on oceanic crust (Fig. 1B; Cedeño et al., 2019). We postulate that an unpenetrated early Aptian source rock (OAE-1A-equivalent) may be present in the deep marine basin (Bihariesingh, 2014), and absent across the Demerara Rise and basin margins. Additionally, along the French Guiana margin, Aptian lacustrine syn-rift deposits may be potential source rock candidates.

Hydrocarbons were extracted from four Lower Cretaceous – Upper Jurassic samples (well A2-1) with very low organic richness (0.11 to 0.43%) yielding very low quantities. It is difficult to determine for certain if the extracts are a naturally occurring product or a drilling introduced contaminant. If the former then their geochemical characteristics are very consistent and would most likely represent the residual product of migratory hydrocarbons rather than in-situ generation. Overall the extracted hydrocarbons are from an aquatic (possibly marine) environment, but with significant terrestrial input (Fig. 9).

To summarise, further geochemical characterisation of the main source rock (Canje Formation) reveals the heterogeneities in age of organic-rich sedimentation, organic richness and kerogen type. Highest TOC with marine Type II kerogen occurs at the Cenomanian-Turonian boundary (OAE-2), typically recognised as a spike in the gamma ray log profile. Free hydrocarbons are recorded throughout all samples analysed in GM-ES-3. Jurassic source potential is not encountered in A2-1, further evidence for its occurrence is postulated. Aptian source rock potential is hypothesised.

ACCEPTED MANUSCRIPT

Downloaded from http://pg.lyellcollection.org/ at University of Manchester, The John Rylands University Library on February 1, 2021

Margin Architecture

Mapping of the deep-penetrating GuyanaSPAN seismic data tied to the re-evaluated wells (Fig. 10) reveals the seismic-stratigraphic architecture of the Guyanas continental margin (Fig. 11; Fig. 12; Fig. 13). Three Mesozoic megasequences are defined and discussed based on our new data (Fig. 2).

Basement

As introduced earlier, the '*basement*' in this study is defined as the crust plus pre- and syn-rift sediments, that exist below the Central Atlantic post-rift succession. Previous studies (Mercier de Lépinay et al., 2016; Reuber et al., 2016; Kusznir et al., 2018) have characterised this interval, which is beyond the scope of this paper. However, a brief overview is provided summarising the evidence for the two models of basement composition. Despite the nature of the basement, the top surface is defined by a major unconformity, interpreted as the top basement (TB), with MS1 strata successively onlapping this surface towards to the southeast (Fig. 12; Fig. 13).

The main evidence for the volcanic nature of the basement below the Demerara Rise is the interpretation of seaward dipping reflectors (SDRs) based on deep-penetrating seismic data (Yang & Escalona, 2011; Mercier de Lépinay et al., 2016; Reuber et al., 2016). Clearly on Fig. 11A, the basement comprises a series of high-amplitude reflections forming a thick package (up to 21 km), dipping towards the Guyana-Suriname basin to the northwest, i.e. seaward dipping. The interpreted basaltic flows have either been associated with the migrating Bahamas hotspot (Morgan, 1983) during early opening of the Central Atlantic (~158 Ma; Reuber et al., 2016), or related to the Central Atlantic Magmatic Province (CAMP) volcanism (~200 Ma; Loncke et al., 2019). Volcanism is further supported by recovered dredge samples of Jurassic-aged (173.4 ± 1.6 Ma) rhyolites and basalts from the Demerara Rise (white star – Fig. 1A; Basile et al., 2020). Additionally, Zinecker & Mann (2020) report SDRs below the conjugate Guinea Plateau.

Megasequence 1 – MS1

Well A2-1 penetrated the deepest and oldest stratigraphy on the Demerara Rise, re-dated as late Tithonian. This succession (up to 7 km thick) of alternating limestone and mudstone forms parallel, high-amplitude reflections (limestones) interspersed with low amplitude, transparent acoustic facies (mudstones) that are extremely laterally continuous (>200 km; Fig. 11A). MS1 and MS2 both prograde basinward towards the northwest. The upper Valanginian MFS (VF) encountered in A2-1 onlaps the TB in a more proximal position (near FG2-1) defining the south-eastern limit of Central Atlantic Ocean during the Lower Cretaceous (Fig. 16A). The MS1 interval is thickest below A2-1, extending below ODP Leg 207 sites (Fig. 12), and temporally records the highest sedimentation rates from the studied wells (Fig. 2). Sediments thin over a series of northeast-trending basement highs and thicken inboard to form an elongate depocentre aligned along the paleo-shelf edge. MS1 sediment is absent northeast of the Guinea-Demerara transform on this map due to succeeding Equatorial Atlantic rifting (now located below the Guinea Plateau) and is notably thin to absent above Jurassic-aged oceanic crust in the Guyana-Suriname basin (Fig. 11A; Fig. 12; Fig. 13).

ACCEPTED MANUSCRIPT

Downloaded from http://pg.lyellcollection.org/ at University of Manchester, The John Rylands University Library on February 1, 2021

Megasequence 2 – MS2

The Valanginian flooding surface (VF) defines the base of MS2, which comprises of a Hauterivian to Aptian-aged mudstone-dominated package, with the top truncated by the BAU across the distal area of the Demerara Rise (Fig. 13). MS2 shows gradual progradation (Fig. 11B) culminating in the major fluvio-deltaic system (Stabroek Formation). Mapping MS2 thickness shows the sequence is completely eroded and peneplaned by the BAU to the north and east against the arcuate-shaped bounding faults of the Demerara Rise (Fig. 12). The pre-Albian northeast-trending anticlinal folds appear to control the amount of erosion, suggesting MS2 was deformed first, followed by peneplanation (Fig. 12). BAU erosion decreases towards the southwest, highlighted along the dip profile (Fig. 11B) and fence diagram (Fig. 13). Towards the present-day South American coastline the sequences below the unconformity are less deformed and no truncation is observed, suggesting a more complete section and the BAU becoming a correlative conformity (Fig. 11B; Mitchum & Vail, 1977). On the north-western margin of the Demerara Rise below the ODP Leg 207 sites, the pre-Albian sediments are rotated by extensional listric normal faults, and thin over a basement high showing compressional features (thrust faults) 100 km downdip in the Guyana-Suriname Basin (Fig. 11A). The extensional domain is divided from the remainder of the Demerara Rise by an arcuate fault zone defining the headwall, positioned above continental crust; the compressional domain is emplaced on Jurassic oceanic crust (Fig. 11A). This feature is interpreted as a major gravitational margin collapse and forms two thick northwest-trending lobes with a spatial extent of over 1000 km^2 emplaced around the basement high (Fig. 13). These lobes (A, B) are observed in strike profile through Fig. 13 separated by a thrusted basement high.

The BAU can be followed through the Guyana-Suriname Basin where overlying sediments onlap this surface. MS2-aged sediments of the French Guiana margin show growth strata into a major basin-bounding eastward-dipping normal fault (Fig. 11A). The thickest MS2 deposits occur along this section of the margin, controlled by accommodation generated in a series of en-échelon normal faults recording the syn-rift non-marine sediments of the proto-Equatorial Atlantic encountered at TD in GM-ES-3 (Fig. 12). These MS2 sequence syn-rift sediments attain maximum thickness in the Brazilian Cacipore grabens (Fig. 15), wells here penetrate >3000 m of non-marine clastics, seismic indicating these rifts attain >6000m thickness (pers. obs). At FG2-1, the basaltic lavas encountered at TD of the well are expressed in the seismic data as a chaotic high amplitude package interpreted to pinch out to the northeast and onlap the basement to the southeast (Fig. 11A). Their distribution forms a north-trending elongate ribbon (Fig. 1B; Gouyet et al., 1994) emplaced above thinned continental crust (Fig. 11A). These breakup volcanics within MS2 are interpreted to be emplaced during Equatorial Atlantic rifting.

Megasequence 3 – MS3

The Late Albian to Maastrichtian MS3 sequence is highly condensed on the northwest of the Demerara Rise, thickening inboard and outboard into the surrounding basins (Fig. 12). These sediments onlap the BAU and gravitational margin collapse, and passively infill the oceanic crust topography beyond the Demerara-Guinea transform in the Equatorial Atlantic (Fig. 12). The remnant topography generated by the gravitational margin collapse is the primary control for MS3 distribution in this area, forming a long-lived sediment depocentre between the two lobes of the gravitational collapse (Fig. 13). A thick depocentre is observed orientated east-west located in the

ACCEPTED MANUSCRIPT

Downloaded from http://pg.lyellcollection.org/ at University of Manchester, The John Rylands University Library on February 1, 2021

south of the study area, related to the location of the palaeo-shelf edge and major sediment input (20.5 Mt/year; Ugwu Oju, 2018) through the shelf-incised Berbice canyon.

An unconformity truncates the stratigraphy in the middle of MS3 (MCU; Fig. 11). In the surrounding basins, erosive incisions at the MCU, hundreds of metres deep, cut into the underlying stratigraphy containing low amplitude fill (Fig. 11A). These are interpreted as the laterally equivalent channel-lobe systems supplying reservoir sands to the recent hydrocarbon discoveries within the Late Cretaceous succession of the Guyana-Suriname Basin, and the Cingulata turbidite fan system in French Guiana. In contrast to the broad topographic relief of the Demerara Rise, the French Guiana margin is much steeper where sediment input is point-sourced at relay zones related to the underlying normal fault array (Fig. 12). The top of the Cretaceous (top MS3) is defined by the BTU across the study area. All these unconformities are more pronounced on the distal area of the Demerara Rise (Fig. 11).

Structural Evolution

Although the structural evolution of the Demerara Rise has been studied before (Gouyet, 1988; Basile et al., 2013; Reuber et al; 2016), important new insights can be developed by employing the new stratigraphic results with deep-penetrating seismic sections, to examine the deformation and basement structure along strike (Fig. 13). Sequential restoration by horizon flattening reveals the structural evolution of the continental margin (Fig. 14).

Angular onlap of the MS1 sequence onto the TB is apparent (Fig. 14D), suggesting significant topography was present prior to deposition of MS1. Flattening on the TB shows the basement was broadly folded prior to of the establishment of the Central Atlantic Jurassic carbonate platform (Fig. 14D). Eventual flooding of the paleo-topography occurred in the upper Valanginian (Fig. 14D). A major depocentre is mapped in MS1 (Fig. 12) positioned above the youngest SDR sequence (syn-6 *sensu* Reuber et al., 2016) that is located between the Jurassic oceanic crust and thinned continental crust, indicating the area of maximum subsidence. MS1 is therefore interpreted to represent fill of accommodation following opening of the Central Atlantic.

The Aptian (125 – 113 Ma) onset of Equatorial Atlantic extension generated syn-rift sinistral en-échelon half grabens along the divergent margin east of the Demerara Rise (Fig. 14C; Pindell, 1985; Greenroyd et al., 2007, 2008a; Basile et al., 2013). On the Demerara Rise, the Equatorial Atlantic rifting induced a transpressional tectonic regime across the northern margin due to movement on the Demerara-Guinea transform. This induced compression buckling of the MS1 and MS2 stratigraphy into tight (wavelength 30-50 km) anticlinal folds trending ENE (Fig. 12). Major imbricate thrust fault systems with hundreds of metres of displacement contain associated roll-overs and basement pop-up structures (Fig. 13). The orientation of these features indicates a maximum paleo-stress direction orientated northwest-southeast suggesting there was significant compression associated with the transpressional Equatorial Atlantic breakup (Fig. 12B). Faulting also affects the underlying basement sequence and is pervasive in the rheologically-competent carbonate lithologies. An approximate estimation of shortening by measuring the most continuous stratigraphic surface (VF) suggests 8.3 km of shortening along the profile orientated in the direction of maximum compression (Fig. 14C).

ACCEPTED MANUSCRIPT

Downloaded from http://pg.lyellcollection.org/ at University of Manchester, The John Rylands University Library on February 1, 2021

Maximum deformation and basin inversion occur localised above the thickest MS1 and MS2 deposits. Deformation continues outboard onto Jurassic oceanic crust (Fig. 13). At this time, there is evidence for gravitational margin collapse to the northwest into the Guyana-Suriname basin induced by uplift-related instability. The compressional features, inversion and gravitational collapse of the margin are all related to transpressional deformation along the sheared northern margin of the Demerara Rise (Gouyet, 1988).

The compression-related paleo-topography was subsequently peneplaned by the BAU across the full width of the Demerara Rise, truncating up to 1 km of section at the A2-1 well location (Fig. 14B), comparable to the amount of erosion observed in the megasequence isochore mapping (Fig. 12). There is a lack of any major incisional features on the peneplaned surface that would be indicative of canyon systems at the resolution of our dataset. The recognition of red oxidised sands in FG2-1 indicates subaerial exposure at this time. Erosion by a combination of subaerial (denudation) and shallow marine submarine processes (wave action) created the peneplain architecture. Eroded sediments are postulated to have filled depocentres adjacent to the Demerara Rise. Accommodation generated by the major bounding fault on the eastern margin of the Demerara Rise forms a significant syn-rift wedge capped by the BAU (Fig. 11A), likely receiving some of the eroded material. Further deformation of the BAU results in the surface subtly tilted to the east and west (Fig. 14A). This deformation is related to the loading of adjacent oceanic crust by the initiation of the Amazon, Essequibo and Orinoco river systems in the Cenozoic depositing excessively thick deep-sea fans, loading the crust and causing subsequent flexure of the Demerara Rise (Watts et al., 2005; Basile et al., 2013).

Chronostratigraphic Analysis

Visualisation in the geological time domain of the stratigraphic architecture can be enhanced through the construction of a Wheeler diagram or chronostratigraphic chart, building a spatiotemporal stratigraphic framework (Wheeler, 1958; Fig. 15). Key stratigraphic surfaces and sequences, re-dated from the samples analysed from seven key wells and scientific boreholes were used as the framework, and later extended to an additional thirteen exploration wells. The Wheeler diagram (Fig. 15) highlights the variability in the age and composition of the basement template as documented earlier. Several wells penetrate continental crust along the margin, with Arapaima-1 (AR-1) recovering phyllitic schists. The Jurassic to Barremian stratigraphy is restricted to below the Demerara Rise based on seismic interpretation (MS1 mapping – Fig. 12) and is only penetrated by A2-1. However, it is conceivable that a condensed equivalent extends out onto the oceanic crust in the Guyana-Suriname basin. Defining the exact age of the Jurassic oceanic crust in the Guyana-Suriname basin is problematic due to the lack of basement penetrations and magnetic anomalies (Nemčok et al., 2017). Based on the east-west spreading axis of the Central Atlantic, it can be assumed oceanic crust becomes younger into the basin towards the northwest.

Further heterogeneity along strike is apparent at the Aptian unconformity. In the Equatorial Atlantic domain, as penetrated by the 1-APS wells, the first deposits within the syn-rift half-grabens are non-marine mudstones, with postulated lacustrine-sourced organic material encountered further along the Equatorial margin (Pasley et al. 2005; Dickson et al., 2016), followed by coarser siliciclastics deposited in fluvial channel and alluvial fan systems of the Cacipore Formation. Contiguous, time-equivalent deposits in the Central Atlantic domain belong to the Stabroek Formation, a unit of

ACCEPTED MANUSCRIPT

Downloaded from http://pg.lyellcollection.org/ at University of Manchester, The John Rylands University Library on February 1, 2021

progradational fluvio-deltaic sands. We assume an Aptian age for the oil-bearing carbonate reservoir encountered in Ranger-1, that built-up above a volcanic seamount in the deep basin. Early Albian Potoco Formation shallow marine limestones, as described from A2-1, are the transgressive deposits that were deposited above the regional BAU. These deposits are restricted to the shallow water areas of the Demerara Rise and Guyana shelf. Time-equivalent shelfal sands are located more proximally (GLO-1 and FG2-1; Fig. 15).

The onset of organic-rich sedimentation is well calibrated at ODP Site 1258C to commence during the late Middle Albian (Fig. 6). Deep-water Late Albian deposition was established in the adjacent French Guiana basin associated with localised turbidites. Marine flooding of this basin and creation of oceanic crust outboard of the GM-ES wells is coincident with the intra Late Albian unconformity recognised across the Demerara Rise (Fig. 6; Fig. 7). The base Cenomanian unconformity truncates the Late Albian stratigraphy along the Guyana shelf and Demerara Rise, coeval with the final continental breakup (unlocking) of the African and South American plates (Geognostics, 2020) at the Demerara Rise-Guinea Plateau. At this time, a short-lived compressional phrase is recognised along the Romanche Fracture Zone within the Equatorial Atlantic (Davison et al., 2016). By earliest Cenomanian times oceanic crust is contiguous between the Central Atlantic and Equatorial Atlantic. Organic-rich sedimentation persists into the Coniacian within the Guyana-Suriname basin and onto the Demerara Rise, forming the prolific source rock of the Canje Formation, and continues even younger into the Upper Santonian further northwest in Venezuela (La Luna facies). Cessation of organic-rich sedimentation is diachronous along the margin, organic levels in FG2-1 decrease during the late Turonian, and even earlier in the early Turonian within the Equatorial Atlantic domain. Subsequent establishment of deep-water turbidite depositional systems, i.e. submarine channel-lobe-fan systems, characterise the Late Cretaceous succession hosting significant oil discoveries within the New Amsterdam Formation.

Deep-water sands overlie the MCU, related to a significant hiatus observed across the Demerara Rise. Although not re-evaluated in this study, several significant unconformities through the Cenozoic are regionally distinguished, often linked to sandstone reservoir development within the overlying sequence (i.e. George Town and Corentyne Formations). Throughout the Cenozoic, shelfal carbonates replace previously siliciclastic-dominated systems, and shallow marine chalks are present over the Demerara Rise.

Palaeogeographical Reconstructions

A series of gross depositional environment (GDE) maps (Fig. 16) have been constructed at four key time intervals during the Cretaceous recognised in the stratigraphic analysis (Fig. 2). These events are either major sequence boundaries or maximum flooding surfaces, representing the environment of deposition during maximum regression or transgression, respectively. Four types of environment are described in this study: terrestrial, transitional, slope, and deep basin with their sand fairways (submarine canyon, channel to fan systems). These environmental interpretations are primarily based on the well data and seismic evidence presented in this study, as well as the incorporation of additional published data. Facies distributions (pies) for wells that penetrate sediments of each age interval are added as control points, however there may be additional penetrations of the stratigraphy unavailable in this study. As the individual depositional systems have been described earlier, a more holistic review of the regional geology is discussed below.

ACCEPTED MANUSCRIPT

Downloaded from http://pg.lyellcollection.org/ at University of Manchester, The John Rylands University Library on February 1, 2021

Upper Valanginian

The conjugate Demerara Rise and Guinea Plateau formed a carbonate-dominated shallow marine embayment extending *ca*. 300 km from the paleo-coastline to the shelf margin. The maximum extent of the south-eastern proto-Central Atlantic Ocean prior to Equatorial Atlantic opening and breakthrough is defined by the coastline shown in Fig. 16A. Due to the gravitational margin collapse, an interpretation of the carbonate shelf margin architecture is restricted, however a carbonate escarpment geometry is documented to the north in The Gambia and to the west in Guyana (Mourlot, 2018; Mourlot et al., 2018; Casson et al., 2020). The extension of the major depocentre below the majority of the Guinea Plateau (Fig. 16A; Zinecker & Mann, 2020) indicates continuous and synchronous deposition linking the conjugate margins, challenging the interpretation by Gouyet et al. (1994) that a local high was present between the Demerara Rise and Guinea Plateau. Lower Cretaceous strata are absent due to post-depositional erosion across the Guyana shelf.

Late Aptian

Rift initiation to the east in the Equatorial Atlantic created an oblique-slip stress regime that exerted transpression-related compression along the Demerara-Guinea transform, leading to the north-westward gravitational collapse of the Demerara Rise margin. A similar gravitational margin collapse feature is recognised from seismic data on the Guinea Plateau (Zinecker & Mann, 2020; Casson et al. *in prep*). The topography generated by this feature on the Guinea Plateau remains reflected in the present-day bathymetry, forming an 'outer high' (Long et al., 2018). Progressive anti-clockwise rotation of Africa away from South America continued to deform the transform margins of the Demerara Rise and Guinea Plateau (Pindell, 1985; Greenroyd et al., 2007, 2008a; Basile et al., 2013). Equatorial Atlantic rifting likely rejuvenated sediment supply from the Guiana Shield resulting in progradation of the fluvio-deltaic systems of the Stabroek Formation (MS2) into the Guyana-Suriname basin. This system was likely fed by a major axial fluvial system interpreted running through the Cacipore Graben north-westwards into French Guiana, with associated non-marine and fluvial sediments preserved within the rifting-induced accommodation. Coastal plain strata are not preserved due to no or low accommodation as recorded in wells I23/-1X, SNY-1 and Tambaredjo (Dronkert & Wong, 1993). Associated exhumation of the hinterland is supported by low-temperature thermochronological data from the northern rim of the Guiana Shield in French Guiana, where Derycke et al. (2018) record a major cooling event suggesting exhumation occurred from 140-100 Ma.

Latest Albian

During this time, elevated organic levels were established in sediments deposited across the shelf to slope environment, evidenced in the studied scientific boreholes. A stepped slope was established along the Guyana-Suriname margin. Deposition of a major submarine channel-fan system was controlled by the antecedent topography generated by the collapsed margin. Rift volcanics observed on seismic are also interpreted throughout the opening Demerara – Guinea oceanic domain segment (Olyphant et al., 2017, Fig. 16C). Adjacent continental margins are narrow and fault-controlled within the extensional basin.

ACCEPTED MANUSCRIPT

Downloaded from http://pg.lyellcollection.org/ at University of Manchester, The John Rylands University Library on February 1, 2021

At this time, models of magnetic anomalies in the oceanic crust (Müller et al., 2008) predict seafloor spreading initiated in the extensional segment offshore French Guiana between 105 and 110 Ma (Albian). The relatively thick (*ca*. 200 m) latest Albian (NC10a oldest) deep marine section documented in GM-ES-3 (Fig. 11A) unconformably, based on seismic interpretation, overlies undated non-marine syn-rift strata. The well is located above thinned continental crust (Fig. 11A). This interval (NC10a) is highly condensed, only 0.55 m thick, on the Demerara Rise above an intra Late Albian unconformity (Fig. 7). We suggest that the creation of accommodation offshore French Guiana and subsequent filling with latest Albian deep marine deposits indicates an early Late Albian age (i.e. pre-intra Late Albian unconformity) for the onset of seafloor spreading and oceanic crust formation. It remains to be understood whether the late Albian marine connection between the Central and Equatorial Atlantic occurred over a flooded Demerara Rise or through an open Demerara-Guinea transform. The conjugated Demerara Rise and Guinea Plateau was likely the final buttress preventing the establishment of a deep-water connection between the Equatorial and Central Atlantic, this deep-water connection was only established with the final phase of oceanic crust formation at the beginning of the Cenomanian, this event is represented by the base Cenomanian unconformity across the Demerara Rise (Fig. 15).

Santonian

By Santonian times (Fig. 16D), Africa has drifted away from South America forming a deep-water connection between North and South Atlantic Oceans. The Late Cretaceous sequence is highly condensed and the MCU is observed in wells across the distal Demerara Rise, due to are remaining as a paleo-high. This period is associated with deposition of extensive submarine fan-channel systems in the basin. These systems offshore French Guiana are relatively narrow ¨å and steep in comparison to their Suriname-Guyana counterparts, perhaps corresponding to the length and volume of the onshore drainage system (Sømme et al., 2009). Entry points for these systems breach relay zones between rift faults along the Equatorial Atlantic margin. The channels of these short systems erode and remove the underlying organic-rich interval as observed in GM-ES-3 (Fig. 3). The deep-water systems in Suriname-Guyana form the prolific hydrocarbon reservoirs encountered in the Stabroek block. Up-dip these systems are fed through the Berbice and Essequibo canyons, depositing sand in submarine channel complexes across the slope to basin floor fans. A re-orientation and retrogression of this fairway axis is observed through the Late Cretaceous, postulated to be related to a decrease in sediment supply through the Berbice canyon and compensational stacking (T_3 – Albian to Turonian; T_4 – Coniacian to Maastrichtian; Mourlot, 2018).

Discussion

Comparison to the Conjugate Margin – Guinea Plateau

Although seismic reflection or well data from the Guinea Plateau was not available for this study, a review of material previously published allows both the conjugate margins to be examined in light of our new findings. Analysis of seismic lines (Fig. 11) on the Demerara Rise, SR1-5400 (GuyanaSPAN), and lines from the Guinea Plateau presented in Edge (2014), reconstructed to their position at pre-Equatorial Atlantic rifting times, i.e. pre-Aptian, reveals that these lines align as ‘conjugates’ (Fig. 16A). This has been used to supplement the GDE mapping of the Guinea Plateau (Fig. 16). Although

ACCEPTED MANUSCRIPT

Downloaded from http://pg.lyellcollection.org/ at University of Manchester, The John Rylands University Library on February 1, 2021

seismic imaging quality of the deep basement structure below the Guinea Plateau is poor, preventing detailed analysis, exploration wells on the southern margin of the Guinea Plateau (GU-2B-1, Sabu-1, Fatala-1; Fig. 16C) targeted the post-rift sequence. Calibration of the oldest strata is extrapolated from wells PGO-2 and PGO-6, reaching TD in Jurassic micritic limestones and shale (Zinecker & Mann, 2020). Notably, both Long et al. (2018) and Zinecker & Mann (2020) during their regional seismic interpretation of 2D seismic data across the Guinea Plateau identified northwest-ward dipping SDR sequences underlying the Jurassic carbonate sequence (~MS1), consistent with the dip orientation of the basement sequence below the Demerara Rise (Reuber et al., 2016). Several major southwest-ward dipping listric faults (i.e. Baraka fault; Fig. 16B) are observed on the southern rifted margin of the Guinea Plateau; Olyphant et al. (2017) interpreted these thick-skinned, sub-vertical faults to penetrate into oceanic basement. These faults within the transform truncate thick crust (i.e. not gradually thinned continental crust as observed on rifted margins). The geometry of the Demerara-Guinea transform faults and narrow conjugate continental margins appear similar, however the first major faults that develop at the continental/oceanic transition have reverse polarities, i.e. the faults near the Guinea Plateau COB dip landward (Zinecker & Mann, 2020), whereas on the Demerara Rise they dip towards the oceanic basin, highlighting the margin asymmetry (Fig. 11B).

Our interpretation is that the mapped Top Neocomian horizon of Edge (2004) represents the Valanginian flooding surface, based on the correlation of seismic facies and architecture (Fig. 11B). Below the base Albian unconformity, the Aptian unconformity and overlying syn-rift wedge is penetrated in well GU-2B-1 on the Guinea Plateau (Fig. 11B). These syn-rift strata are only preserved basinward of the east-west trending Baraka fault (see Fig. 3 in Olyphant et al., 2017), likely analogous to the syn-rift strata offshore French Guiana (Fig. 11A) and correlating with the pre-Albian Cacipore Formation in the Foz do Amazonas basin (Fig. 15). Within this sequence, breakup related basalts and volcaniclastics are penetrated in wells GU-2B-1 and Sabu-1 (Olyphant et al., 2017), distributed along the southern margin of the Guinea Plateau (Fig. 16C; Benkhelil et al., 1994; Gouyet et al., 1994). The apparent lack of any Aptian compressional deformation on the conjugate margin seismic profile (Fig. 11B) is probably due to its position, as the majority of the deformation is located on the southwest nose of the Guinea Plateau (Fig. 16B; cf. Zinecker & Mann, 2020). There is a considerable difference in the Cenozoic sediment thickness (Fig. 11B); progradational sigmoidal seismic reflections (clinoforms) on the Demerara Rise indicate the deposition of a major shelfal siliciclastic system penetrated in well GLO-1 leading to the deeper burial of pre-Cenozoic stratigraphy.

Margin Heterogeneity Influenced by Structural Inheritance

Evaluating the margin architecture at a super-regional scale, i.e. >1000 km along strike, highlights the heterogeneities that result in the segmentation of continental margins (e.g. Watts & Stewart, 1998; Franke et al., 2007; Faleide et al., 2008). From this study, spatial variabilities are recorded in the depositional systems (Fig. 16), associated drainage systems onshore, structural style (Fig. 13; Fig. 14) and organic matter distribution (Fig. 9). Further studies show segmentation causes additional variations in subsidence history (Pereira & Alves, 2011; Tsikalas et al. 2001). Sedimentation over the Demerara Rise, particularly the more distal section, is heavily condensed with low sedimentation rates (Fig. 2), and many Cretaceous to recent post-rift unconformities are recorded (Fig. 11). These re-dated surfaces are interpreted to be sequence boundaries developed at lowstands that can be

ACCEPTED MANUSCRIPT

Downloaded from http://pg.lyellcollection.org/ at University of Manchester, The John Rylands University Library on February 1, 2021

correlated with increased siliciclastic delivery into the adjacent deep-water basins (Vail et al., 1980). Additionally, the margins of the Demerara Rise were the focus of repeated tectonic deformation, developing both transpressional and extensional fault systems, during Equatorial Atlantic breakup (Fig. 16). Internal deformation of the Demerara Rise is diverse, ranging from broad long-wavelength folding to tight imbricate thrust fault systems (Fig. 13). Fundamentally the stratigraphic and structural heterogeneities discussed are consequential of the pre-rift structural inheritance, eventually modified by the dual-phase rifting history.

The Demerara Rise and its conjugate, the Guinea Plateau, is thought to have formed a focal point for hot spot magmatism (CAMP or Bahamas hotspot related) during the early stages of the Central Atlantic opening, potentially creating a volcanic accumulation up to 21 km thick (Reuber et al., 2016; Long et al., 2018; Zinecker Mann, 2020). These submarine plateaus are clearly identifiable in present-day bathymetric maps, being a testament to the longstanding influence this basement configuration had on the bathymetry and ultimately, the segmentation of the continental margin, as observed on other TMPs worldwide (Loncke et al., 2019). The location of the volcanism in the south-eastern Central Atlantic has been interpreted as creating a 'pinning point' for the final fragmentation of Gondwana and the breakup of the Equatorial Atlantic segment (Pindell, 1985; Greenroyd et al., 2007, 2008a; Basile et al., 2013). It is conceivable the Jurassic volcanism created a crustal weakness exploited during the second Equatorial phase of rifting. Similar segmentation of continental margins and its effects on post-rift deposition are documented globally from the rifted Norwegian (Tsikalas et al. 2001), western India (Calvès et al., 2011), Levant (Ben-Avraham et al., 2006) and Uruguayan margins (Soto et al., 2001).

Conclusions

New stratigraphic analysis by re-sampling seven exploration wells and scientific boreholes located along the Guyanas continental margin of South America has been used to refine a high-resolution Jurassic to Cretaceous stratigraphic framework, applicable to the Central Atlantic. This framework is applied to the interpretation of a margin-scale two-dimensional deep seismic reflection survey to produce a new megasequence architectural model, create updated paleogeographic reconstructions for four key geological intervals and reconstruct the structural evolution through the two divergent phases of breakup during the Jurassic (Central Atlantic) and Cretaceous (Equatorial Atlantic).

Our findings highlight deposition during the early Central Atlantic post-rift sequence (Jurassic-Lower Cretaceous i.e. MS1) was influenced by the underlying heterogenous basement structure, composed of thinned continental crust and volcanic addition in the form of thick SDR sequences. The major MS1 depocentre below the Demerara Rise that continues below the conjugate Guinea Plateau passively infilled pre-existing basement topography. The only well on the South American margin to penetrate this sequence is the A2-1 well. New multi-proxy biostratigraphy data conclusively reveals the well reached total depth in late Tithonian organic-lean (average TOC 0.37%) shales and limestones. Previous work that suggests A2-1 penetrated a Jurassic-aged source rock is questioned by this new integrated dataset. MS1 is capped by a super-regional maximum flooding surface (MFS) during the upper Valanginian (VF) recognised elsewhere around the Central Atlantic and Gulf of Mexico. The landward limit of the MFS reveals the south-eastern extension of the early Central Atlantic.

ACCEPTED MANUSCRIPT

Downloaded from http://pg.lyellcollection.org/ at University of Manchester, The John Rylands University Library on February 1, 2021

Rifting in the Equatorial Atlantic during Barremian to Aptian times modified the continental margin architecture, the structure and succeeding depositional systems. Deep pre-Albian grabens formed along the proto-Equatorial margins receiving continental sedimentation. Further associated breakup volcanism is evidenced by 125 Ma basalts recovered in the French Guiana FG2-1 well. The progressive anti-clockwise rotation of Africa from South America during the Aptian induced a transpressional regime causing an estimated 8.3 km of shortening across the distal Demerara Rise. This tectonism resulted in short-wavelength folding and thrusting, major gravitational margin collapse into adjacent basins and the formation of a progradational shelfal siliciclastic system (Stabroek Formation). This sequence (MS2) is truncated by a super-regional angular unconformity re-dated as basal Albian (BAU), peneplaning up to 1 km of sediment from the Demerara Rise.

At GM-ES-3, the rapid facies change from rifted continental deposits into Late Albian deep water deposits is a possible reflection of the creation of oceanic crust outboard in the extensional segment of the opening Equatorial Atlantic offshore French Guiana and associated rapid subsidence of the basin margin. This event is represented by the time synchronous intra Late Albian unconformity recognised on the Demerara Rise. ,. Our model suggests final breakup of the Demerara Rise and Guinea Plateau, and deep marine connection between the Equatorial and Central Atlantic occurred during the earliest Cenomanian following unlocking of the Demerara-Guinea transform.

The distal Demerara Rise sedimentary sequence is highly condensed and contains multiple unconformities dated as middle Campanian (MCU), base Tertiary (BTU) and middle Miocene (MMU), suggesting this area remained an area of low accommodation and a relative high likely due to the anonymously thick crust. Onset of organic-rich sedimentation (Canje Formation) co-occurred with the flooding of the Equatorial Atlantic (pre-oceanic crust formation), during the late Middle Albian. Geochemical characterisation of these primarily marine Type II organic-rich strata (average TOC 4.21%) shows heterogeneity along strike, reflecting sediment dilution and terrestrial organic matter input.

The topography generated by the gravitational margin collapse is interpreted to have been a major control on the entry point of siliciclastic delivery, funnelling sediment from the shallow Demerara Rise into the deep-water sedimentary systems of the Guyana-Suriname basin. The Berbice canyon has already been described from previous studies as another major sediment input point throughout the Late Cretaceous, delivering sediment to the world-class hydrocarbon reservoirs in the Guyana-Suriname basin. Coeval siliciclastic input occurred along the Equatorial margin, and the depositional systems display relatively short runout lengths, related to the steep, narrow margin geometry.

Examining the sedimentary systems using this integrated approach at a margin-scale reveals the important control of inherited pre-rift structural and basement heterogeneity, and later structural evolution associated with the second phase of breakup, on the post-rift depositional system distribution and overall margin heterogeneity.

ACCEPTED MANUSCRIPT

Acknowledgements

This study is part of the lead authors PhD project at the University of Manchester. We thank the sponsoring companies of the North Africa Research Group (NARG) for their continued financial and scientific support. The sampling and subsequent analysis of DSDP/ODP cores was partially supported

Downloaded from http://pg.lyellcollection.org/ at University of Manchester, The John Rylands University Library on February 1, 2021

by a European Consortium for Ocean Research Drilling (ECORD) research grant awarded to the lead author. Holger Kuhlmann provided excellent support during our visits to the Bremen Core Repository and subsequent requests for additional samples. Shell is thanked for the access to hydrocarbon exploration well data, particularly Tyrone Sigur at the CGG storage facility, Schulenburg, Texas. Iain Prince and Peter Osterloff (Shell) are thanked for their attentive support and additionally David Owen and Robert Campbell (Shell) helped improve the manuscript. The seismic data presented is courtesy of ION Geophysical. Ian Mounteney is acknowledged for his assistance in performing the XRD analysis at the British Geological Survey, Keyworth. Alastair Bewsher at the University of Manchester is thanked for use of the organic geochemistry laboratory. Discussion with Jon Teasdale and academic access to the Geognostics Earth Model (GEM™) were particularly useful in understanding the regional geology, plate tectonics and structure. Frédéric de Ville de Goyet thanks Nick Miles, Petrostrat for assistance in the Lower Cretaceous palynology. Daniela Reháková was supported by the VEGA 2/2013/20 Project. Prof. David Wray, Greenwich University is acknowledged for his assistance running the pyrolysis. Cairn Energy are thanked for funding the hydrocarbon extractions at GeoMark Research. Jim Armstrong is acknowledged for his assistance interpreting the organic geochemistry results. Aruna Mannie (Premier Oil) and Paul Mann (University of Houston) are thanked for their constructive reviews that improved the clarity of this paper.

Figure Captions

Fig. 1 (A) – Shaded bathymetric and topographic location map of northeast South America showing the structure of the Guyanas continental margin and subsurface dataset. Exploration wells and scientific boreholes used in this study are shown; orange circles highlight where new stratigraphic analysis has been performed. The ION Geophysical GuyanaSPAN 2D seismic reflection survey, the location of the composite seismic section (Fig. 11A), dip section SR1-5400 (Fig. 11B) and the isochore maps are shown (Fig. 12). Dredge samples recovered basalts and rhyolites zircon-dated at 173.4 ± 1.6 Ma (Basile et al., 2020) from the seabed (white star). Onshore, the limit of sedimentary cover and hence the location of the Archean Guiana Shield is mapped (Cordani et al., 2016). Hydrocarbon discoveries and the limits of Cretaceous source kitchens after Kosmos (2018). DR – Demerara Rise; WA – Waini Arch. (B) – Structural framework of the Guyanas continental margin with a top basement depth structure map interpreted from the ION Geophysical GuyanaSPAN 2D seismic reflection survey. The 'top basement' map was constructed from a merge between the top oceanic crust and top basement surfaces. The onshore geological map is from the Geological Map of South America (CGMW, CPRM, DNPM, 2003). Structural features are mapped after Gouyet et al. (1994), Yang and Escalona (2011), Reuber et al. (2016), Sapin et al. (2016), crustal thickness modelled from 3D gravity anomaly inversion by Kusznir et al. (2018), predicted Jurassic graben offshore (Griffith, 2017), and volcanics from Gouyet et al. (1994) and Mourlot (2018).

Fig. 2 – Tectono-stratigraphic framework for the Guyanas continental margin, offshore Suriname and Guyana. The major sequence stratigraphic surfaces identified in this study are indicated, linked to key biostratigraphy events. Lithostratigraphy is based on seismic profile SR1-5400 (Fig. 11B) and adapted from Nemčok et al. (2016), key in Fig. 15. The main seismic markers and megasequences used in this study are highlighted. Calculated sedimentation rates (sedi-rates) displayed in metres per million years (m/Myr). Relative sea level curve after Haq (2014). AF – Albian flooding surface; CAMP – Central Atlantic Magmatic Province; CF – Cenomanian flooding surface; OAE – oceanic anoxic event; SDRs – seaward dipping reflectors; TB – top basement.

Fig. 3 – A re-evaluation of the Guiana-Maritime GM-ES-3 well stratigraphy displaying nannofossil events (**Error! Reference source not found.**), total organic carbon (TOC; **Error! Reference source not found.**) measurements and key stratigraphic surfaces. Location displayed on Fig. 1A.

ACCEPTED MANUSCRIPT

Downloaded from http://pg.lyellcollection.org/ at University of Manchester, The John Rylands University Library on February 1, 2021

Fig. 4 – A re-evaluation of the French Guiana 2-1 (FG2-1) well stratigraphy displaying nannofossil events (**Error! Reference source not found.**), foraminifera and palynology results, total organic carbon (TOC; **Error! Reference source not found.**) measurements and key stratigraphic surfaces. Location displayed on Fig. 1A.

Fig. 5 – A re-evaluation of the Demerara A2-1 well stratigraphy displaying nannofossil events (**Error! Reference source not found.**), foraminifera and palynology results, total organic carbon (TOC; **Error! Reference source not found.**) measurements and key stratigraphic surfaces. Oil shows indicated on lithology column as green stars. Palynology abbreviations: CMN – common, FDCO – first downhole common occurrence. Location displayed on Fig. 1A.

Fig. 6 – A re-evaluation of the ODP Leg 207 Site 1258C stratigraphy displaying nannofossil events (**Error! Reference source not found.**), total organic carbon (TOC; **Error! Reference source not found.**) data compiled from Meyers et al. (2006) and key stratigraphic surfaces. A 12 m correction has been applied to the gamma ray log, where LD is logger's depth and DD is driller's depth. Early Late Albian ammonites identified in cores 30 and 31 by Owen & Mutterlose (2006) are annotated, as well as the cores displayed in Fig. 7. Location displayed on Fig. 1A.

Fig. 7 – Photographs of two cores, 15 and 27 from ODP Leg 207 Site 1258C with analysed samples and interpreted ages displayed by red arrows, highlighting the Cretaceous stratigraphy and unconformities present in the borehole (Erbacher et al., 2004a). Inset – zoom in on the sharp contact between the calcareous nannofossil clay of Unit 3 and black shale of Unit 4 representing the middle Campanian unconformity (MCU) and a ca. 12 Myr hiatus (Erbacher et al., 2004b). Ceno. – Cenomanian; Camp. – Campanian. Scale in cm.

Fig. 8 – A re-evaluation of the DSDP Leg 14 Site 144 stratigraphy displaying nannofossil events (**Error! Reference source not found.**), total organic carbon (TOC; **Error! Reference source not found.**) measurements and key stratigraphic surfaces. Location displayed on Fig. 1A.

Fig. 9 – Classification of kerogen types using hydrogen and oxygen indices plotted on a modified van Krevelen diagram displaying the results of the Rock-Eval pyrolysis. The symbology reflects the age of each sample analysed. New data generated in this study from four of the revised wells (A2-1, DSDP Site 144, FG2-1 and GM-ES-3) is amalgamated with data presented in Meyers et al. (2006) from ODP Site 1258C, the ages are updated following the new biostratigraphy results. The tabulated data is presented in the supplementary material (**Error! Reference source not found.**).

Fig. 10 – Synthetic seismogram calculated for two exploration wells, Demerara A2-1 (Fig. 5) and French Guiana FG2-1 (Fig. 4), providing the well to seismic correlation of key horizons and megasequences identified in this new stratigraphic study. Extracted statistical wavelets presented. Location of the two wells displayed on Fig. 1A.

Fig. 11 (A) – Composite seismic section in depth displaying megasequence architecture along a >1000 km length of the Guyanas continental margin. Location displayed on Fig. 1A. Erosional truncation (red arrows) and onlap (black arrows) marked. BFF – basin floor fan; MFS – maximum flooding surface. (B) – Conjugate dip-orientated seismic depth sections from the Demerara Rise (2D line – SR1-5400, clipped at 20 km depth) and Guinea Plateau (after Edge, 2014) displaying megasequence architecture. Location displayed on Fig. 1A and reconstructed location on Fig. 16A. Note change of horizontal and vertical scale from (A). COB – continent-ocean boundary. Seismic data courtesy of ION Geophysical.

Fig. 12 – Isochore thickness maps for three megasequences, MS1 – top basement (seaward dipping reflectors, continental and oceanic crust) to upper Valanginian maximum flooding surface (VF); MS2 – VF to base Albian unconformity (BAU); MS3 – BAU to base Tertiary unconformity (BTU). Cont. – continental; GP – Guinea Plateau; TJ – top Jurassic.

Fig. 13 – A fence diagram constructed from 7 dip-orientated (N-S) seismic depth sections across the Demerara Rise, interpreted with the megasequences, structural domains and underlying basement

ACCEPTED MANUSCRIPT

Downloaded from http://pg.lyellcollection.org/ at University of Manchester, The John Rylands University Library on February 1, 2021

structure. BAU – Base Albian unconformity; COB – continent-ocean boundary. Seismic data courtesy of ION Geophysical. Location inset.

Fig. 14 – Sequential restoration by horizon flattening for a segment of the strike seismic profile displayed in Fig 11A, at three key time stages, (D) Valanginian, (C) Aptian and (B) Albian revealing the structural evolution of the continental margin to (A) present day. A zoom in on the seismic around Demerara A2-1 with a projection of the uppermost truncated seismic reflection (black dashed line) revealing approximately a kilometre of erosion at the well location is shown. MFS – maximum flooding surface. Fig. 1A for location of the section.

Fig. 15 – A Wheeler diagram constructed along strike from Guyana (left) to Brazil (right) detailing the stratigraphic evolution of the segmented Guyanas continental margin. Pin stripe vertical lines indicate hiatus' corresponding to various regional unconformities dated in the stratigraphic analysis. Dash black and white lines indicate revised wells in this study. The geological time scale (GTS 2018) is non-linear. Hydrocarbon occurrences are shown. Average TOC values for the Canje Formation displayed, AR-1 data from Mourlot (2018).

Fig. 16 – Gross depositional environment (GDE) maps for four key time stages, defined by the stratigraphic analysis, in the evolution of the Guyanas continental margin. (A) Upper Valanginian (135 Ma); (B) Aptian (115 Ma); (C) Latest Albian (101 Ma) and (D) Santonian (85 Ma). The reconstructed location of the conjugate seismic sections (Fig. 11B) are displayed in (A). Facies distribution (%) for the interval encountered in each well is shown. Geometries were reconstructed following the Geognostics Earth Model (GEM™). BFF – basin floor fan; DR – Demerara Rise; FZ – fracture zone; GP – Guinea Plateau.

References

Allen, P.A. and Allen, J.R., 2013. Basin analysis: Principles and application to petroleum play assessment. John Wiley & Sons.

Ando, A., Huber, B.T., MacLeod, K.G. and Watkins, D.K., 2015. Early Cenomanian "hot greenhouse" revealed by oxygen isotope record of exceptionally well-preserved foraminifera from Tanzania. Paleoceanography, 30(11), pp.1556-1572.

Armstrong, H., Brasier, M., 2013. Microfossils. John Wiley & Sons.

Bally, A.W., 1981. Atlantic-type margins, pp.1-48.

Basile, C., Girault, I., Paquette, J.L., Agranier, A., Loncke, L., Heuret, A. and Poetisi, E., 2020. The Jurassic magmatism of the Demerara Plateau (offshore French Guiana) as a remnant of the Sierra Leone hotspot during the Atlantic rifting. Scientific Reports, 10(1), pp.1-12.

Basile, C., Mascle, J. and Guiraud, R., 2005. Phanerozoic geological evolution of the Equatorial Atlantic domain. Journal of African Earth Sciences, 43(1-3), pp.275-282.

Basile, C., Maillard, A., Patriat, M., Gaullier, V., Loncke, L., Roest, W., De Lepinay, M.M. and Pattier, F., 2013. Structure and evolution of the Demerara Plateau, offshore French Guiana: Rifting, tectonic inversion and post-rift tilting at transform–divergent margins intersection. Tectonophysics, 591, pp.16-29.

Behar, F., Beaumont, V. and Penteado, H.D.B., 2001. Rock-Eval 6 technology: performances and developments. Oil & Gas Science and Technology, 56(2), pp.111-134.

Below, R., 1982: Scolochorate Zysten der Gonyaulacaceae (Dinophyceae) aus der Unterkreide Marokkos. Palaeontographica, Abteilung B, v.182, p.1-51, pl.1-9.

Ben-Avraham, Z., Schattner, U., Lazar, M., Hall, J.K., Ben-Gai, Y., Neev, D. and Reshef, M., 2006. Segmentation of the Levant continental margin, eastern Mediterranean. Tectonics, 25(5).

ACCEPTED MANUSCRIPT

Downloaded from http://pg.lyellcollection.org/ at University of Manchester, The John Rylands University Library on February 1, 2021

Benkhelil, J., Mascle, J. and Tricart, P., 1995. The Guinea continental margin: an example of a structurally complex transform margin. Tectonophysics, 248(1-2), pp.117-137.

Bland, S., Griffiths, P. and Hodge, D., 2004. Restoring the seismic image with a geological rule base. first break, 22(4).

Bown, P., 1998. Calcareous nannofossil biostratigraphy. Chapman and Hall; Kluwer Academic, pp.1–315.

Bown, P.R, Rutledge, D., Crux, J.A. and Gallagher, L.T., 1998. Lower Cretaceous. In Bown, P. (Ed.), Calcareous Nannofossil Biostratigraphy. (pp. 86-131). Chapman and Hall; Kluwer Academic.

Bown, P.R., 2001. Calcareous nannofossils of the Gault, Upper Greensand and Glauconitic Marl (Middle Albian-Lower Cenomanian) from the BGS Selborne boreholes, Hampshire. Proceedings of the Geologists' Association, 112(3), pp.223-236.

Bralower, T.J., Sliter, W.V., Arthur, M.A., Leckie, M.R., Allard, D. and Schlanger, S.O., 1993. Dysoxic/Anoxic Episodes in the Aptian-Albian (Early Cretaceous). The Mesozoic Pacific. Geology, Tectonics and Volcanism. Geophysical Monograph 77, American Geophysical Union, 5-37.

Burk, K. and Dewey, J.F., 1974. Two plates in Africa during the Cretaceous?. Nature, 249(5455), pp.313-316.

Burnett, J.A., 1998. Upper Cretaceous. In Bown, P.R. (ed.), Calcareous nannofossil biostratigraphy: Dordrecht, The Netherlands (Kluwer Academic Publishers), 132-199.

Calvès, G., Schwab, A.M., Huuse, M., Clift, P.D., Gaina, C., Jolley, D., Tabrez, A.R. and Inam, A., 2011. Seismic volcanostratigraphy of the western Indian rifted margin: The pre-Deccan igneous province. Journal of Geophysical Research: Solid Earth, 116(B1).

Casson, M.A., Calves, G., Redfern, J., Huuse, M. and Sayers, B., 2020. Cretaceous continental margin evolution revealed using quantitative seismic geomorphology, offshore northwest Africa. Basin Research.

Casson et al. 2020 in prep. A stratigraphic re-evaluation of key Central Atlantic DSDP sites.

Cedeño, A.F., Ohm, S.E., Escalona, A. and Narain, E. 2019. Petroleum System (S?) in the Guyana-Suriname Basin: Insights from a Geochemical Study Onshore Suriname. European Association of Geoscientists & Engineers Conference Proceedings, 29th International Meeting on Organic Geochemistry, Sep 2019, pp.1 – 2.

CGMW, CPRM, DNPM, 2003. 1: 5,500,000 Geological Map of South America. Commission for the Geological Map of the World (CGMW), Geological Survey of Brazil (CPRM), National Department of Mineral Production, Brazil (DNPM). CD-ROM.

Charton, R.J.G., 2018. Phanerozoic Vertical Movements in Morocco. (Doctoral dissertation). TUDelft, Netherlands.

Clemson, J., Cartwright, J. and Booth, J., 1997. Structural segmentation and the influence of basement structure on the Namibian passive margin. Journal of the Geological Society, 154(3), pp.477-482.

Cordani, U.G., Ramos, V.A., Fraga, L.M., Delgado, I., de Souza, K.G., Gomes, F.E.M, Schobbenhaus, C., and Cegarra, M. 2016. Tectonic map of South America. Commission for the geological map of the world.

Costa, L. I. & Davey, R. J., 1992. Dinoflagellate Cysts of the Cretaceous System. In: A Stratigraphic Index of Dinoflagellate Cysts, Ed. by A. J. McIntyrepowel (Chapman and Hall, London), 99–131.

Davey, R.J., 1982: Dinocyst stratigraphy of the latest Jurassic to Early Cretaceous of the Haldager No. 1 borehole, Denmark. Danmarks Geologiske Undersøgelse, Series B, 6, 1-57, pl.1-10.

ACCEPTED MANUSCRIPT

Downloaded from http://pg.lyellcollection.org/ at University of Manchester, The John Rylands University Library on February 1, 2021

Davison, I., Faull, T., Greenhalgh, J., Beirne, E.O. and Steel, I., 2016. Transpressional structures and hydrocarbon potential along the Romanche Fracture Zone: a review. Geological Society, London, Special Publications, 431(1), pp.235-248.

Derycke, A., Gautheron, C.., Bourbon, P., Pinna-Jamme, R., Aertgeerts, G., Simon-Labric, T., 2018. French Guyana margin evolution: insight by low-temperature thermochronological data.

Dickson, W., Schiefelbein, C.F., Odegard, M.E. and Zumberge, J.E., 2016. Petroleum systems asymmetry across the South Atlantic Equatorial Margins. Geological Society, London, Special Publications, 431(1), pp.219-233.

Dodekova, L., 1969: Dinoflagellés et acritarches du Tithonique aux environs de Pleven, Bulgarie central du nord. Bulgarska Akademiya na Naukite, Izvestiya na Geologicheskiya Institut, Seriya Paleontologiya, v.18, p.13-24, pl.1-5.

Doyle, J. A., Jardiné, S. & Doerenkamp, A., 1982. Afropollis, a new genus of early angiosperm pollen, with notes on the Cretaceous palynostratigraphy and paleoenvironments of Northern Gondwana. Bulletin des Centres Recherches Exploration-Production Elf Aquitaine, 6, 39–117.

Dronkert, H. and Wong, T.E., 1993. Geology of the Tambaredjo oil field, Suriname. AAPG Bulletin (American Association of Petroleum Geologists, United States), 77 (CONF-930306).

Duxbury, S. 1983. A study of dinoflagellate cysts and acritarchs from the Lower Greensand (Aptian to Lower Albian) of the Isle of Wight, southern England. Palaeontographica Abt. B, 186; 18-80.

Edge, R., 2014. Rifting of the Guinea Margin in the Equatorial Atlantic from 112 to 84 MA: Implications of Paleo-reconstructions for Structure and Sea-surface Circulation. Ph.D Thesis. Retrieved from. http://hdl.handle.net/10150/321395.

Erbacher, J., Mosher, D.C. and Malone, M.J., et al. 2004a. Demerara Rise; equatorial Cretaceous and Paleogene paleoceanographic transect, western Atlantic; covering Leg 207 of the cruises of the drilling vessel JOIDES Resolution; Bridgetown, Barbados, to Rio de Janeiro, Brazil; Sites 1257–1261; 11 January–6 March 2003, in M. Chapman, and L. L. Peters, eds., Proceedings of the Ocean Drilling Program (ODP), Initial Reports, Part A-207: Texas A&M University, pp.1–89.

Erbacher, J., Mosher, D.C. and Malone, M.J., et al. 2004b. Site 1258, in M. Chapman, and L. L. Peters, eds., Proceedings of the Ocean Drilling Program (ODP), Initial Reports, Part A-207: Texas A&M University.

Erbacher, J., Friedrich, O., Wilson, P.A., Birch, H. and Mutterlose, J., 2005. Stable organic carbon isotope stratigraphy across Oceanic Anoxic Event 2 of Demerara Rise, western tropical Atlantic. Geochemistry, Geophysics, Geosystems, 6(6).

Erlich, R. N., Villamil, T., and Keens-Dumas, J., 2003. Controls on the deposition of Upper Cretaceous organic carbon–rich rocks from Costa Rica to Suriname, in C. Bartolini, R. T. Buffler, and J. Blickwede, eds., The Circum-Gulf of Mexico and the Caribbean: Hydrocarbon habitats, basin formation, and plate tectonics: AAPG Memoir 79, pp.1–45.

Faleide, J.I., Tsikalas, F., Breivik, A.J., Mjelde, R., Ritzmann, O., Engen, O., Wilson, J. and Eldholm, O., 2008. Structure and evolution of the continental margin off Norway and the Barents Sea. Episodes, 31(1), pp.82-91.

Fanget, A.S., Loncke, L., Pattier, F., Marsset, T., Roest, W.R., Tallobre, C., de Madron, X.D. and Hernández-Molina, F.J., 2020. A synthesis of the sedimentary evolution of the Demerara Plateau (Central Atlantic Ocean) from the Late Albian to the Holocene. Marine and Petroleum Geology, 114, p.104-195.

Figueiredo, J.J.J.P., Hoorn, C., Van der Ven, P. and Soares, E., 2009. Late Miocene onset of the Amazon River and the Amazon deep-sea fan: Evidence from the Foz do Amazonas Basin. Geology, 37(7), pp.619-622.

ACCEPTED MANUSCRIPT

Downloaded from http://pg.lyellcollection.org/ at University of Manchester, The John Rylands University Library on February 1, 2021

Flügel, E., 2004. Depositional models, facies zones and standard microfacies. In Microfacies of Carbonate Rocks (pp. 657-724). Springer, Berlin, Heidelberg.

Franke, D., 2013. Rifting, lithosphere breakup and volcanism: Comparison of magma-poor and volcanic rifted margins. Marine and Petroleum geology, 43, pp.63-87.

Franke, D., Neben, S., Ladage, S., Schreckenberger, B. and Hinz, K., 2007. Margin segmentation and volcano-tectonic architecture along the volcanic margin off Argentina/Uruguay, South Atlantic. Marine Geology, 244(1-4), pp.46-67.

Friedrich, O. and Erbacher, J., 2006. Benthic foraminiferal assemblages from Demerara Rise (ODP Leg 207, western tropical Atlantic): possible evidence for a progressive opening of the Equatorial Atlantic Gateway. Cretaceous Research, 27(3), pp.377-397.

Gale, A.S., Bown, P., Caron, M., Crampton, J., Crowhurst, S.J., Kennedy, W.J., Petrizzo, M.R. and Wray, D.S., 2011. The uppermost Middle and Upper Albian succession at the Col de Palluel, Hautes-Alpes, France: An integrated study (ammonites, inoceramid bivalves, planktonic foraminifera, nannofossils, geochemistry, stable oxygen and carbon isotopes, cyclostratigraphy). Cretaceous Research, 32, pp.59-130.

Garzanti, E., 2016. From static to dynamic provenance analysis—Sedimentary petrology upgraded. Sedimentary Geology, 336, pp.3-13.

Gasperini, L., Bernoulli, D., Bonatti, E., Borsetti, A.M., Ligi, M., Negri, A., Sartori, R. and Von Salis, K., 2001. Lower Cretaceous to Eocene sedimentary transverse ridge at the Romanche Fracture Zone and the opening of the equatorial Atlantic. Marine Geology, 176(1-4), pp.101-119.

Geognostics 2020. Geognostics Eart Model (GEM).

Gouiza, M., Bertotti, G., Charton, R., Haimoudane, K., Dunkl, I. and Anczkiewicz, A.A., 2019. New Evidence of Anomalous Vertical Movements along the Hinterland of the Atlantic NW African Margin. Journal of Geophysical Research: Solid Earth.

Gouyet, S., 1988. Evolution tectono-sédimentaire des marges guyanaise et nord-brésilienne au cours de l'ouverture de l'Atlantique Sud (Doctoral dissertation).

Gouyet, S., Unternehr, P. and Mascle, A., 1994. The French Guyana margin and the Demerara Plateau: geological history and petroleum plays. In Hydrocarbon and petroleum geology of France (pp. 411-422). Springer, Berlin, Heidelberg.

Grabowski, J., Lakova, I., Petrova, S., Stoykova, K., Ivanova, D., Wójcik-Tabol, P., Sobień, K. and Schnabl, P., 2016. Paleomagnetism and integrated stratigraphy of the Upper Berriasian hemipelagic succession in the Barlya section Western Balkan, Bulgaria: Implications for lithogenic input and paleoredox variations. Palaeogeography, Palaeoclimatology, Palaeoecology, 461, pp.156-177.

Greenroyd, C.J., Peirce, C., Rodger, M., Watts, A.B. and Hobbs, R.W., 2007. Crustal structure of the French Guiana margin, west equatorial Atlantic. Geophysical Journal International, 169(3), pp.964-987.

Greenroyd, C.J., Peirce, C., Rodger, M., Watts, A.B. and Hobbs, R.W., 2008a. Crustal structure and evolution of the Demerara Plateau, French Guiana: Geophysical Journal International, 172, pp.549–564,

Greenroyd, C. J., Peirce, C., Rodger, M., Watts, A.B. and Hobbs, R.W. 2008b. Demerara Plateau — The structure and evolution of a transform passive margin: Geophysical Journal International, 172, pp.549–564.

Griffith, C.P., 2017. Evidence for a Jurassic Source Rock in the Guiana-Suriname Basin. AAPG Datapages/Search and Discovery Article #90291, AAPG Annual Convention and Exhibition, Houston, Texas, April 2-5, 2017.

ACCEPTED MANUSCRIPT

Downloaded from http://pg.lyellcollection.org/ at University of Manchester, The John Rylands University Library on February 1, 2021

Habib, D. & Drugg, W.S. 1983. Dinoflagellate age of Middle Jurassic-Early Cretaceous sediments in the Blake-Bahama Basin. Deep Sea Drilling Project, Washington, Initial reports, 76: 623-638.

Hardas, P. and Mutterlose, J., 2006. Calcareous nannofossil biostratigraphy of the Cenomanian/ Turonian boundary interval of ODP Leg 207 at the Demerara Rise. Revue de micropaléontologie 49. pp. 165–179.

Haq, B.U., 2014. Cretaceous eustasy revisited. Global and Planetary change, 113, pp.44-58.

Hardas, P. and Mutterlose, J., 2006. Calcareous nannofossil biostratigraphy of the Cenomanian/Turonian boundary interval of ODP Leg 207 at the Demerara Rise. Revue de micropaléontologie, 49(3), pp.165-179.

Hayes, D.E., Pimm, A.C., Beckman, J.B., Benson, W.E., Berger, W.H., Roth, P.H., Supko, P.R., and von Rad, U., 1972. Initial reports of the Deep Sea Drilling Project. US Government Printing office. Washington DC, 14, pp.975.

Heine, C., Zoethout,J. and Müller, R. D., 2013. Kinematics of the South Atlantic rift. Solid Earth Discussions, 5, pp.41– 116.

Hill, M.E., 1976. Lower Cretaceous calcareous nannofossils from Texas and Oklahoma. Palaeontographica Abteilung B, 156, 4-6, pp.103-179.

Jacobi, R.D. and Hayes, D.E., 1982. Bathymetry, microphysiography and reflectivity characteristics of the West African margin between Sierra Leone and Mauritania. In Geology of the Northwest African continental margin (pp. 182-212). Springer, Berlin, Heidelberg.

James, R., Scotchman, J. & Head, R., 2020. Why is there heavy oil in Cenozoic reservoirs offshore Guyana. Halliburton exploration insights, April, 2020.

Jeremiah, J., 1996. A proposed Albian to lower Cenomanian nannofossil biozonation for England and the North Sea Basin. Journal of Micropalaeontology 15 (2), pp.97–129.

Jeremiah, J., 2001. A Lower Cretaceous nannofossil zonation for the North Sea Basin. Journal of Micropalaeontology, 20, pp. 45-80.

Kneller, E.A. and Johnson, C.A., 2011. Plate kinematics of the Gulf of Mexico based on integrated observations from the Central and South Atlantic. Gulf Coast Association of Geological Societies Transactions, 61, pp.283–299.

Kulhanek, D.K. and Wise, S.W. Jr., 2006. Albian calcareous nannofossils from ODP Site 1258, Demerara Rise. Revue de Micropaléontologie 49, pp. 181-195.

Kosmos Energy, 2018. Investor Presentation – March 2018. Dallas, Texas. Available from <https://www.kosmosenergy.com/>.

Krauspenhar, P.M., Carvalho, M.A., Fauth, G. and Lana, C.C., 2014. Albian Palynostratigraphy of ODP Leg 207 (Holes 1257A, 1258C and 1260B), Demerara Rise, Equatorial Atlantic. Revue de micropaléontologie, 57(1), pp.1-13.

Kulhanek, D.K. & Wise, S.W., 2006. Albian calcareous nannofossils from ODP Site 1258, Demerara Rise. Revue de micropaléontologie, 49, pp. 181-195.

Kusznir, N.J., Roberts, A.M. and Alvey, A.D., 2018. Crustal structure of the conjugate Equatorial Atlantic Margins, derived by gravity anomaly inversion. Geological Society, London, Special Publications, 476, pp.SP476-5.

Labails, C., Olivet, J.L., Aslanian, D. and Roest, W.R., 2010. An alternative early opening scenario for the Central Atlantic Ocean. Earth and Planetary Science Letters, 297(3-4), pp.355-368.

Loncke, L., Roest, W.R., Klingelhoefer, F., Basile, C., Graindorge, D., Heuret, A., Marcaillou, B., Museur, T., Fanget, A.S. and de Lépinay, M.M., 2019. Transform marginal plateaus. Earth-Science Reviews, p.102940.

ACCEPTED MANUSCRIPT

Downloaded from http://pg.lyellcollection.org/ at University of Manchester, The John Rylands University Library on February 1, 2021

Long, A., Cameron, N. and Sayers, B., 2018. The Guinea Marginal Plateau: Correlations from Seismic and Potential Fields. In AAPG Europe Regional Conference, Global Analogues of the Atlantic Margin.

Loucks, R.G., Kerans, C., Zeng, H. and Sullivan, P.A., 2017. Documentation and characterization of the Lower Cretaceous (Valanginian) Calvin and Winn carbonate shelves and shelf margins, onshore northcentral Gulf of Mexico. The American Association of Petroleum Geologists Bulletin, v. 101 (1), pp. 119–142.McCoss, A. 2017. Opening New Oil Basins: A Pattern of Discoveries. In AAPG Annual Convention and Exhibition. Search and Discovery Article #70280.

McKenzie, D., 1978. Some remarks on the development of sedimentary basins. Earth and Planetary science letters, 40(1), pp.25-32.

Mercier de Lépinay, M., Loncke, L., Basile, C., Roest, W.R., Patriat, M., Maillard, A. and De Clarens, P., 2016. Transform continental margins–Part 2: A worldwide review. Tectonophysics, 693, pp.96-115.

Meyers, P.A., Bernasconi, S.M. and Forster, A., 2006. Origins and accumulation of organic matter in expanded Albian to Santonian black shale sequences on the Demerara Rise, South American margin. Organic Geochemistry, 37(12), pp.1816-1830.

Mitchum, R.M. and Vail, P.R., 1977. Seismic Stratigraphy and Global Changes of Sea Level: Part 7. Seismic Stratigraphic Interpretation Procedure: Section 2. Application of Seismic Reflection Configuration to Stratigraphic Interpretation.

Monteil, E. 1992. Kystes de dinoflagelles index (Tithonique-Valanginien) du Sud-Est de la France. Proposition d'une nouvelle zonation palynologique. Revue de Paleobilogie, 11: 299-306.

Morgan, W.J., 1983. Hotspot tracks and the early rifting of the Atlantic. In Developments in Geotectonics (Vol. 19, pp. 123-139). Elsevier.

Mosher, D., Erbacher, J., Zuelsdorff, L. and Meyer, H., 2005. Stratigraphy of the Demerara Rise, Suriname, South America: a rifted margin, shallow stratigraphic source rock analogue. In American association of petroleum geologists annual meeting, Calgary.

Moulin, M., Aslanian, D. and Unternehr, P., 2010. A new starting point for the South and Equatorial Atlantic Ocean. Earth-Science Reviews, 98(1-2), pp.1-37.

Mourlot, Y., 2018. Contrôles sur la répartition des argiles organiques dans les bassins profonds: cas de l'Atlantique central au Crétacé (Doctoral dissertation, Université de Toulouse, Université Toulouse III-Paul Sabatier).

Mourlot, Y., Calvès, G., Clift, P.D., Baby, G., Chaboureau, A.C. and Raisson, F., 2018. Seismic stratigraphy of Cretaceous eastern Central Atlantic Ocean: Basin evolution and palaeoceanographic implications. Earth and Planetary Science Letters, 499, pp.107-121.

Müller, R.D., Sdrolias, M., Gaina, C. and Roest, W.R., 2008. Age, spreading rates, and spreading asymmetry of the world's ocean crust. Geochemistry, Geophysics, Geosystems, 9(4).

Nemčok, M., Rybár, S., Ekkertová, P., Kotulová, J., Hermeston, S.A. and Jones, D., 2016. Transform-margin model of hydrocarbon migration: the Guyana–Suriname case study. Geological Society, London, Special Publications, 431(1), pp.199-217.

Olyphant, J.R., Johnson, R.A. and Hughes, A.N., 2017. Evolution of the Southern Guinea Plateau: Implications on Guinea-Demerara Plateau formation using insights from seismic, subsidence, and gravity data. Tectonophysics, 717, pp.358-371.

Owen, H.G. and Mutterlose, J., 2006. Late Albian ammonites from offshore Suriname: implications for biostratigraphy and palaeobiogeography. Cretaceous Research, 27(6), pp.717-727.

ACCEPTED MANUSCRIPT

Downloaded from http://pg.lyellcollection.org/ at University of Manchester, The John Rylands University Library on February 1, 2021

Pasley, M.A., Shepherd, D.B., Pocknall, D.T., Boyd, K.P., Andrade, V. and Figueiredo, J.P., 2004, October. Sequence stratigraphy and basin evolution of the Foz do Amazonas Basin, Brazil. In AAPG ICE (p. 12).

Payton, C.E. ed., 1977. Seismic stratigraphy: applications to hydrocarbon exploration (Vol. 26, pp. 1-516). Tulsa, OK: American Association of Petroleum Geologists.

Pereira, R. and Alves, T.M., 2011. Margin segmentation prior to continental breakup: A seismic–stratigraphic record of multiphased rifting in the North Atlantic (Southwest Iberia). Tectonophysics, 505(1-4), pp.17-34.

Pindell, J.L., 1985. Alleghenian reconstruction and subsequent evolution of the Gulf of Mexico, Bahamas, and proto-Caribbean. Tectonics, 4(1), pp.1-39.

Reháková, D, and Michalík, J, 2000. Calcareous dinoflagellate and calpionellid bioevents versus sea-level fluctuations recorded in the West-Carpathian (Late Jurassic/Early Cretaceous) pelagic environments. Geologica Carpathica, 51(4), pp.229-243.

Reuber, K.R., Pindell, J. and Horn, B.W., 2016. Demerara Rise, offshore Suriname: Magma-rich segment of the Central Atlantic Ocean, and conjugate to the Bahamas hot spot. Interpretation, 4(2), pp.141-155.

Sapin, F., Davaux, M., Dall'Asta, M., Lahmi, M., Baudot, G. and Ringenbach, J.C., 2016. Post-rift subsidence of the French Guiana hyper-oblique margin: from rift-inherited subsidence to Amazon deposition effect. Geological Society, London, Special Publications, 431(1), pp.125-144.

Schlanger, S.O., Arthur, M.A., Jenkyns, H.C. and Scholle, P.A., 1987. The Cenomanian-Turonian Oceanic Anoxic Event, I. Stratigraphy and distribution of organic carbon-rich beds and the marine δ13C excursion. Geological Society, London, Special Publications, 26(1), pp.371-399.

Sheriff, R.E., 1976. Inferring stratigraphy from seismic data. AAPG Bulletin, 60(4), pp.528-542.

Sheriff, R.E., 1977. Limitations on Resolution of Seismic Reflections and Geologic Detail Derivable from Them: Section 1. Fundamentals of Stratigraphic Interpretation of Seismic Data.

Sibuet, J.C. and Mascle, J., 1978. Plate kinematic implications of Atlantic equatorial fracture zone trends. Journal of Geophysical Research: Solid Earth, 83(B7), pp.3401-3421.

Snyder, R.L. and Bish, D.L. 1989. Quantitative analysis. In: Bish, D.L., Post, J.E. (Eds), Modern Powder Diffraction, Reviews in Mineralogy, Volume 20, Mineralogical Society of America, USA, pp. 101-144 (Chapter 5).

Sømme, T.O., Helland-Hansen, W., Martinsen, O.J. and Thurmond, J.B., 2009. Relationships between morphological and sedimentological parameters in source-to-sink systems: a basis for predicting semi-quantitative characteristics in subsurface systems. Basin Research, 21(4), pp.361-387.

Soto, M., Morales, E., Veroslavsky, G., de Santa Ana, H., Ucha, N. and Rodríguez, P., 2011. The continental margin of Uruguay: Crustal architecture and segmentation. Marine and Petroleum Geology, 28(9), pp.1676-1689.

Staatsolie, Suriname National Oil Company, 2013. Suriname International Competitive Bid Round, http://www.staatsolie.com/pio/images/stories/PDF/suriname_international_bidding_round2013.pdf.

Stonecipher, S.A., 1999. Genetic Characteristics of Glauconite and Siderite: Implications for the Origin of Ambiguos Isolated Marine Sandbodies.

Tallobre, C., Loncke, L., Bassetti, M.A., Giresse, P., Bayon, G., Buscail, R., de Madron, X.D., Bourrin, F., Vanhaesebroucke, M. and Sotin, C., 2016. Description of a contourite depositional system on

ACCEPTED MANUSCRIPT

Downloaded from http://pg.lyellcollection.org/ at University of Manchester, The John Rylands University Library on February 1, 2021

the Demerara Plateau: Results from geophysical data and sediment cores. Marine Geology, 378, pp.56-73.

Thibault, N. and Gardin, S., 2006. Maastrichtian calcareous nannofossil biostratigraphy and paleoecology in the Equatorial Atlantic (Demerara Rise, ODP Leg 207 Hole 1258A). Revue de micropaléontologie, 49(4), pp.199-214.

Tsikalas, F., Faleide, J.I. and Eldholm, O., 2001. Lateral variations in tectono-magmatic style along the Lofoten–Vesterålen volcanic margin off Norway. Marine and Petroleum Geology, 18(7), pp.807-832.

Ugwu-Oju, O., 2018. Clinothems of the Cretaceous Berbice Canyon, Offshore Guyana (Doctoral dissertation, Colorado School of Mines. Arthur Lakes Library).

Vail, P.R., Mitchum, R.M., Shipley, T.H. and Buffler, R.T., 1980. Unconformities of the North Atlantic. Philosophical Transactions of the Royal Society of London. Series A, Mathematical and Physical Sciences, 294(1409), pp.137-155.

van Helden, B.G.T., 1986. Dinoflagellate cysts at the Jurassic-Cretaceous boundary, offshore Canada. Palynology, 10:181-199.

Watkins, D. K. and Bowdler, J.L., 1984. Cretaceous calcareous nannofossils from Deep Sea Drilling Project Leg 77, Southeast Gulf of Mexico. In: Buffler, R.T; Schlager, W. et al. (eds.). Initial Reports of the Deep-Sea Drilling Project, Washington (U.S. Govt. Printing Office), 77, pp. 659-674.

Watkins, D.K., Cooper, M.J., and Wilson, P.A., 2005. Calcareous nannoplankton response to late Albian oceanic anoxic event 1d in the western North Atlantic. Paleoceanography, Vol. 20, PA2010, pp. 1-14.

Watts, A.B. and Stewart, J., 1998. Gravity anomalies and segmentation of the continental margin offshore West Africa. Earth and Planetary Science Letters, 156(3-4), pp.239-252.

Watts, A.B., Rodger, M., Peirce, C., Greenroyd, C.J. and Hobbs, R.W., 2009. Seismic structure, gravity anomalies, and flexure of the Amazon continental margin, NE Brazil. Journal of Geophysical Research: Solid Earth, 114(B7).

Wheeler, H. E. 1958. Time-stratigraphy. American Association of Petroleum Geologists Bulletin, 42, pp.1047–1063.

Wilson, J.T., 1966. Did the Atlantic close and then re-open? Nature, 211(5050), pp.676-681.

Yang, W. and Escalona, A., 2011. Tectonostratigraphic evolution of the Guyana Basin. AAPG bulletin, 95(8), pp.1339-1368.

Zinecker, M.P. and Mann, P., 2020 *in press*. Mesozoic to recent tectonostratigraphy, paleogeography, and hydrocarbon prospectivity of the Guinea Plateau, northwestern Africa. Journal of Marine and Petroleum Geology.

ACCEPTED MANUSCRIPT

Downloaded from http://pg.lyellcollection.org/ at University of Manchester, The John Rylands University Library on February 1, 2021

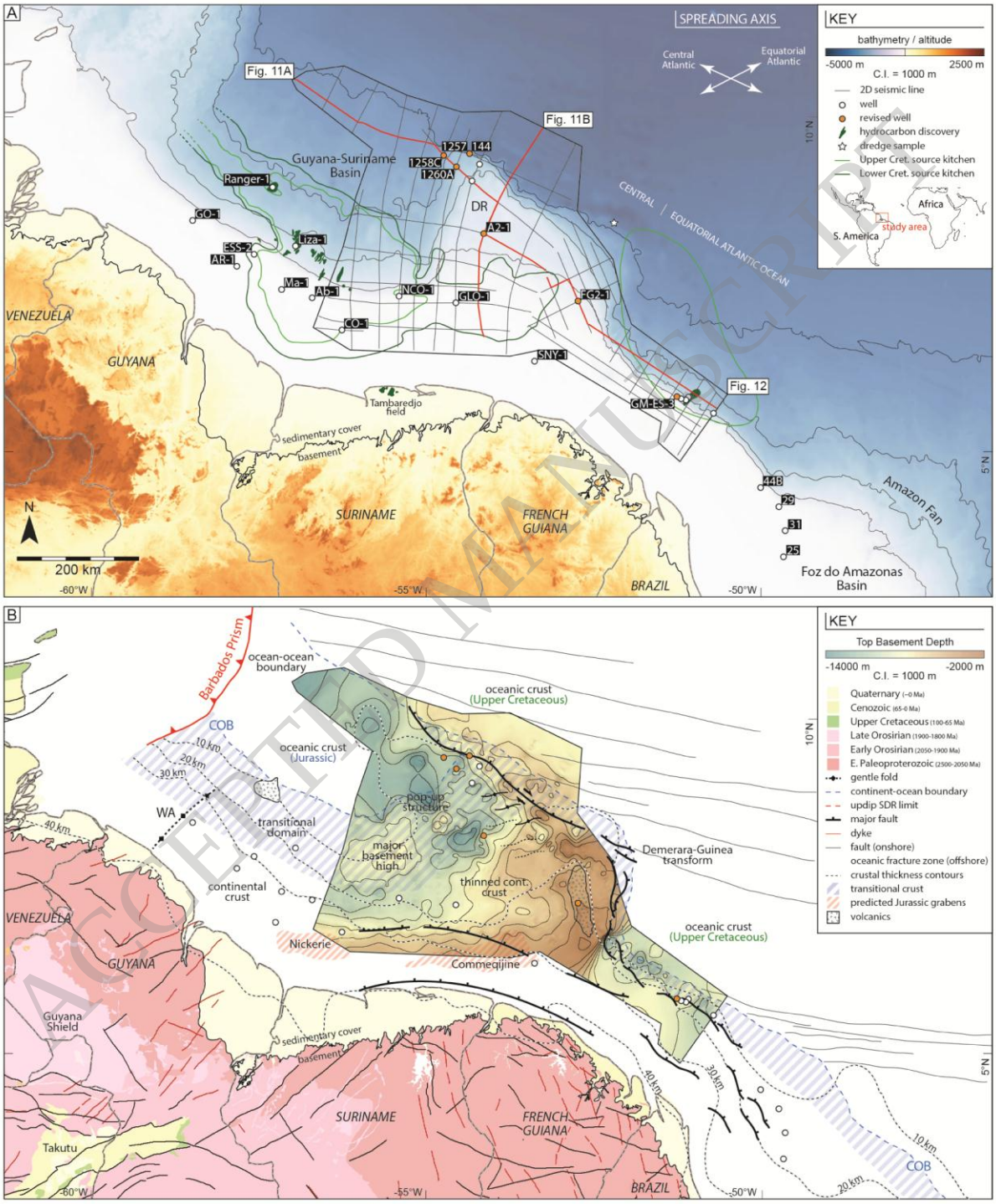

ACCEPTED MANUSCRIPT

Downloaded from http://pg.lyellcollection.org/ at University of Manchester, The John Rylands University Library on February 1, 2021

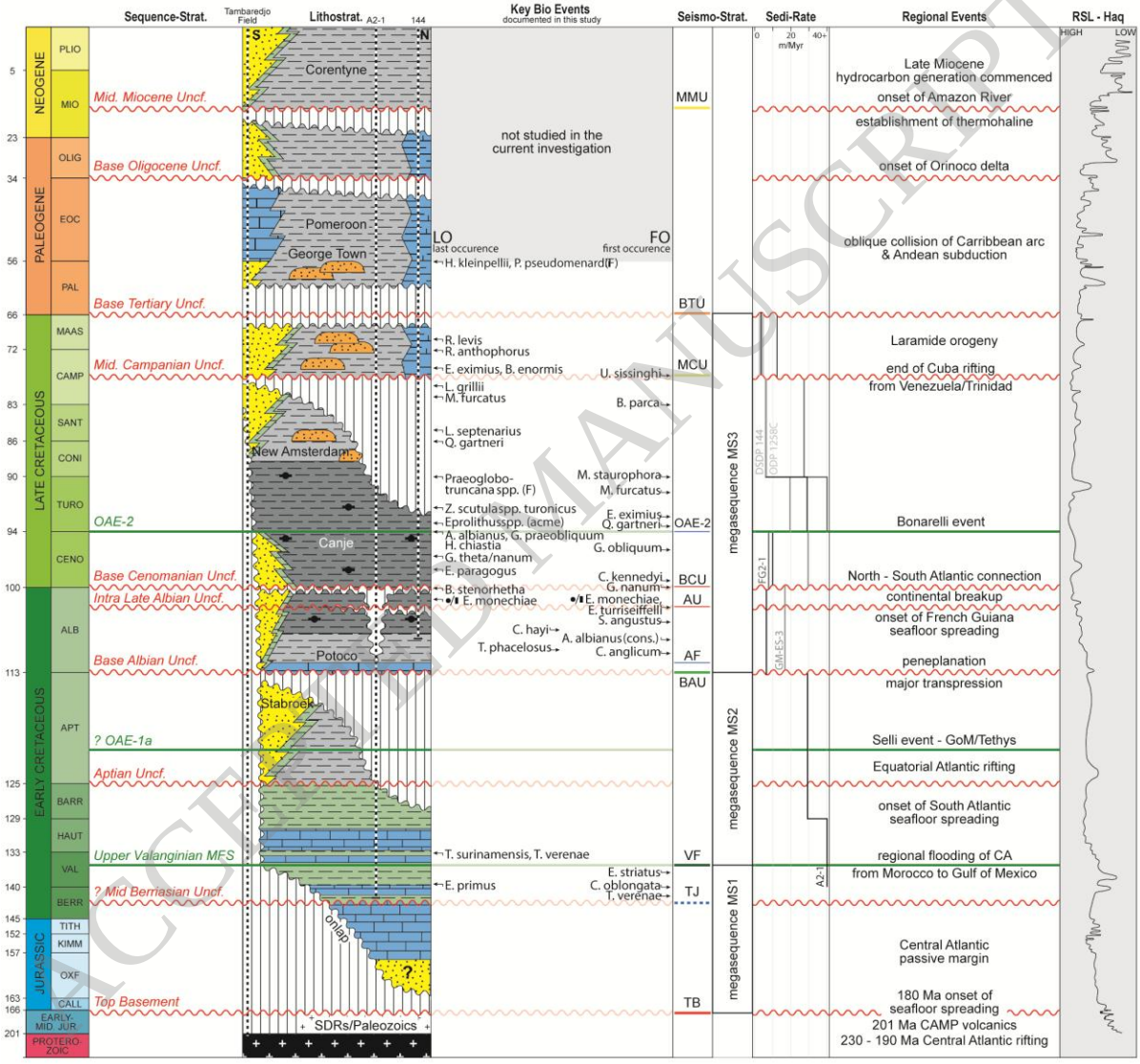

ACCEPTED MANUSCRIPT

Downloaded from http://pg.lyellcollection.org/ at University of Manchester, The John Rylands University Library on February 1, 2021

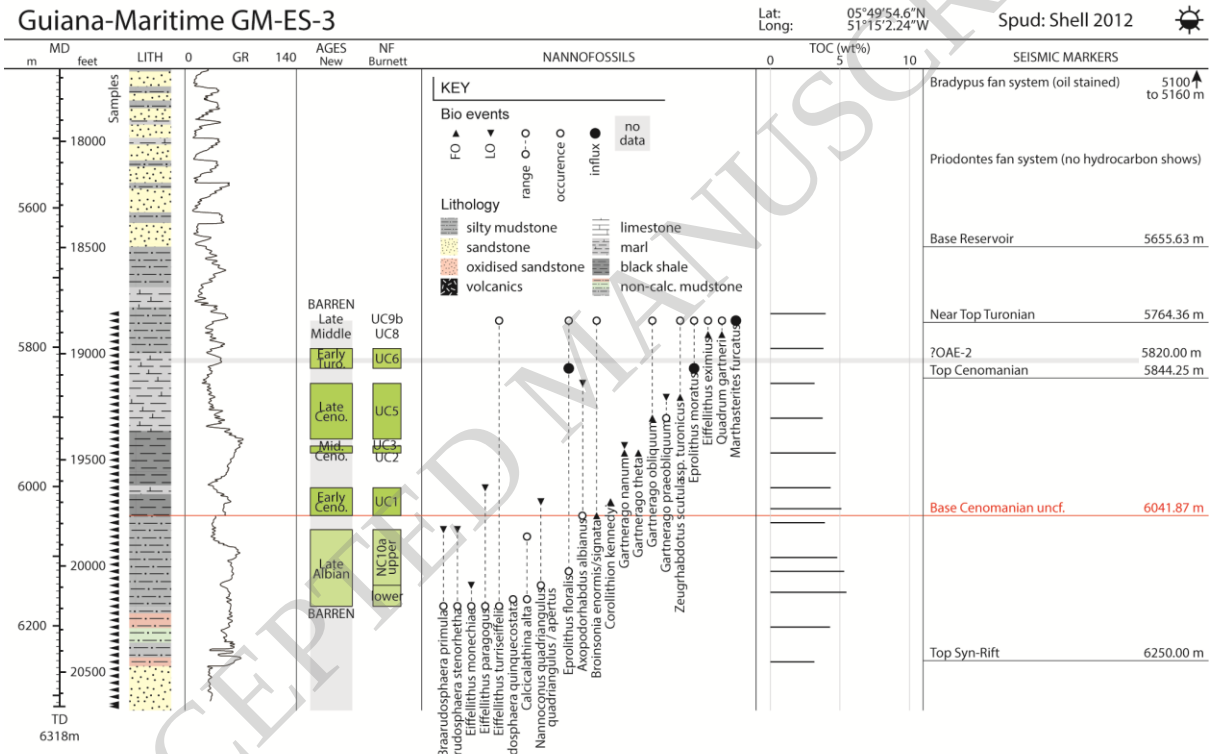

ACCEPTED MANUSCRIPT

Downloaded from http://pg.lyellcollection.org/ at University of Manchester, The John Rylands University Library on February 1, 2021

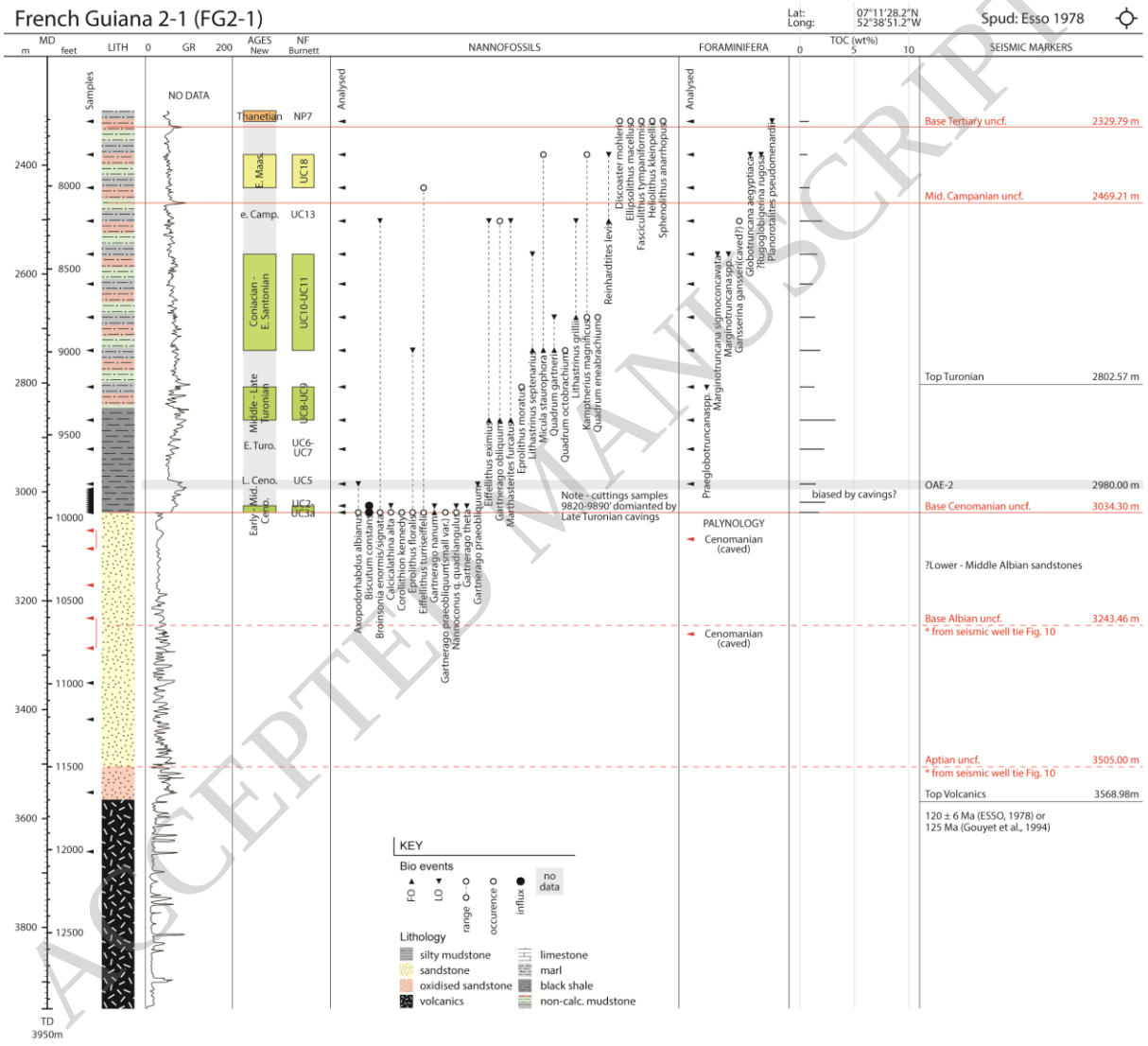

ACCEPTED MANUSCRIPT

Downloaded from http://pg.lyellcollection.org/ at University of Manchester, The John Rylands University Library on February 1, 2021

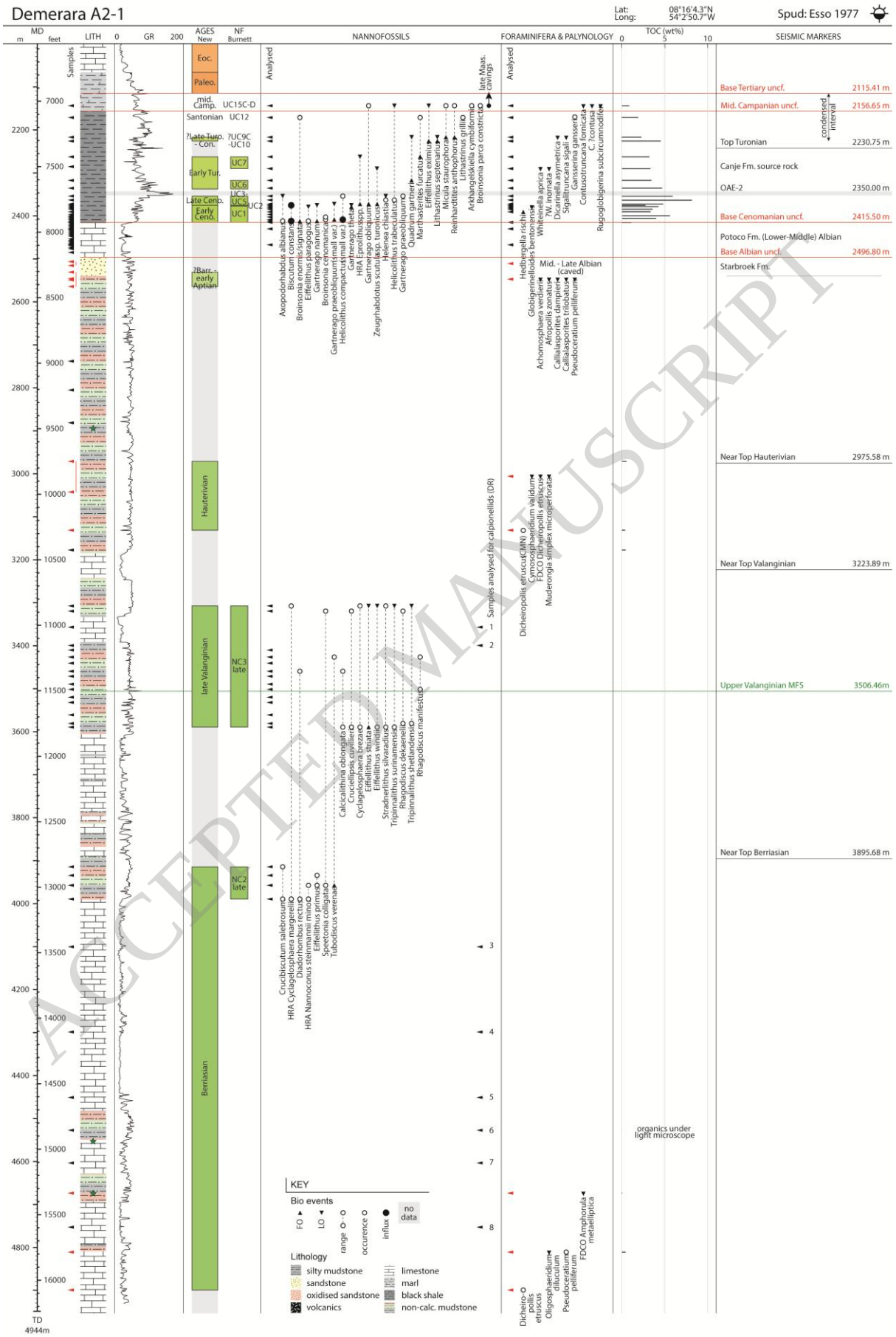

ACCEPTED MANUSCRIPT

Downloaded from http://pg.lyellcollection.org/ at University of Manchester, The John Rylands University Library on February 1, 2021

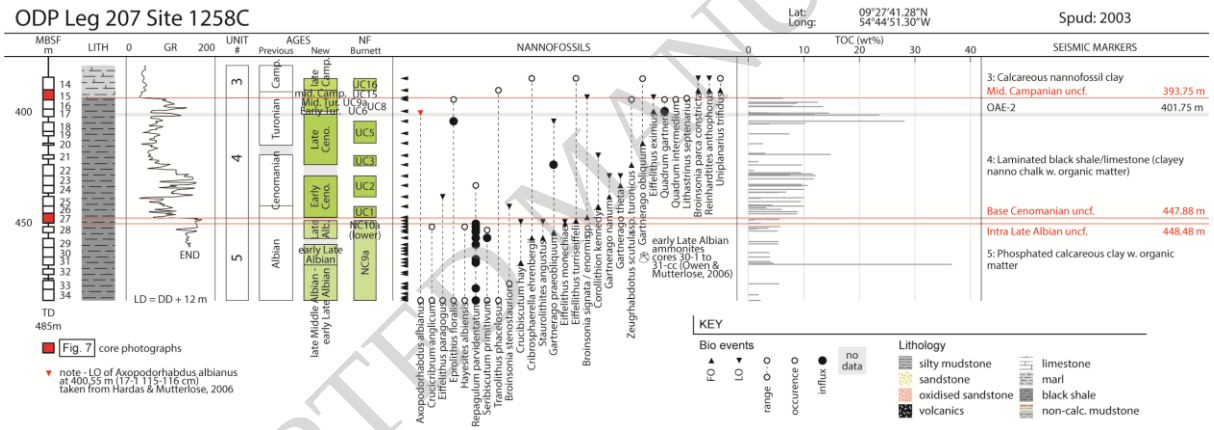

ACCEPTED MANUSCRIPT

Downloaded from http://pg.lyellcollection.org/ at University of Manchester, The John Rylands University Library on February 1, 2021

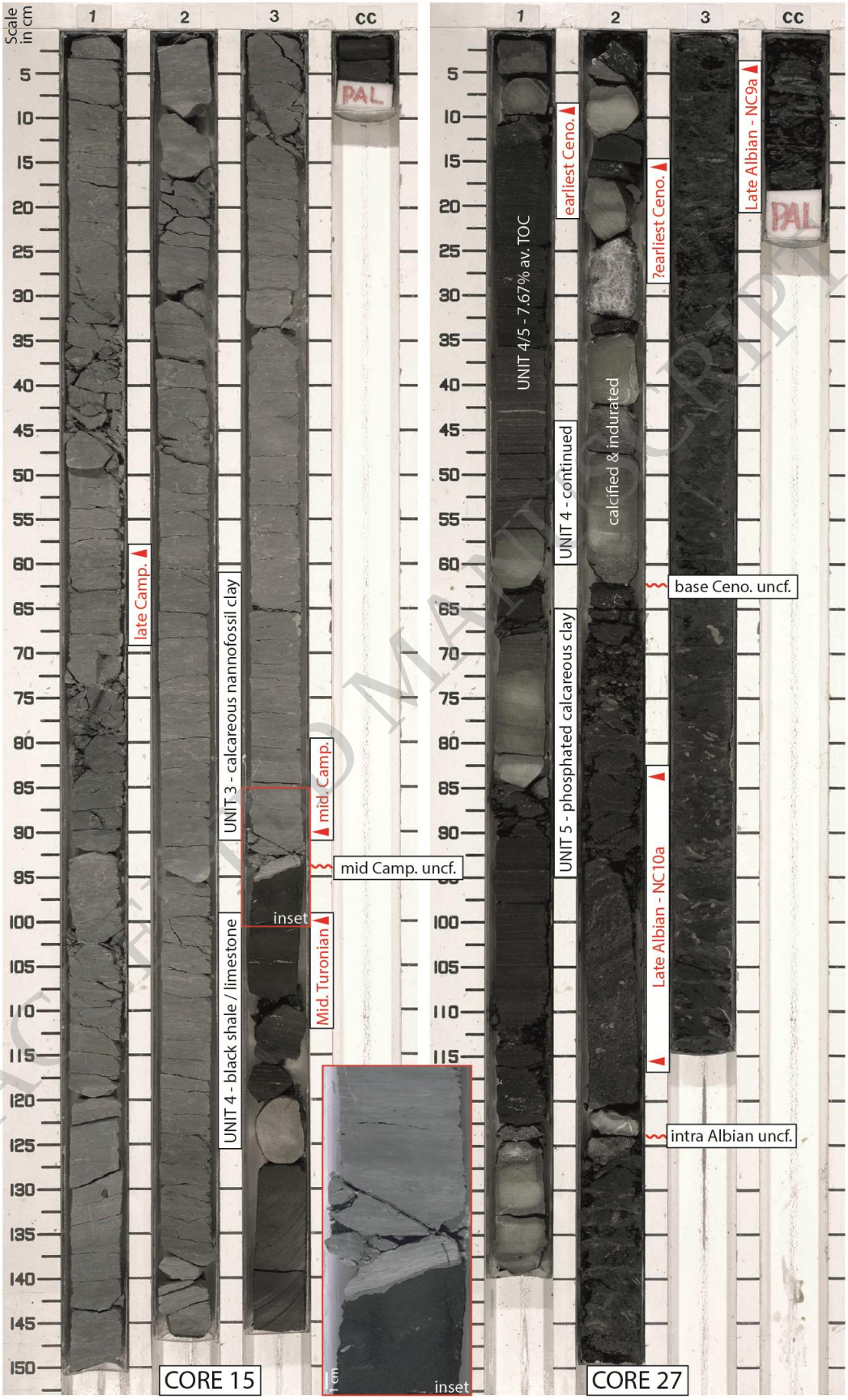

ACCEPTED MANUSCRIPT

Downloaded from http://pg.lyellcollection.org/ at University of Manchester, The John Rylands University Library on February 1, 2021

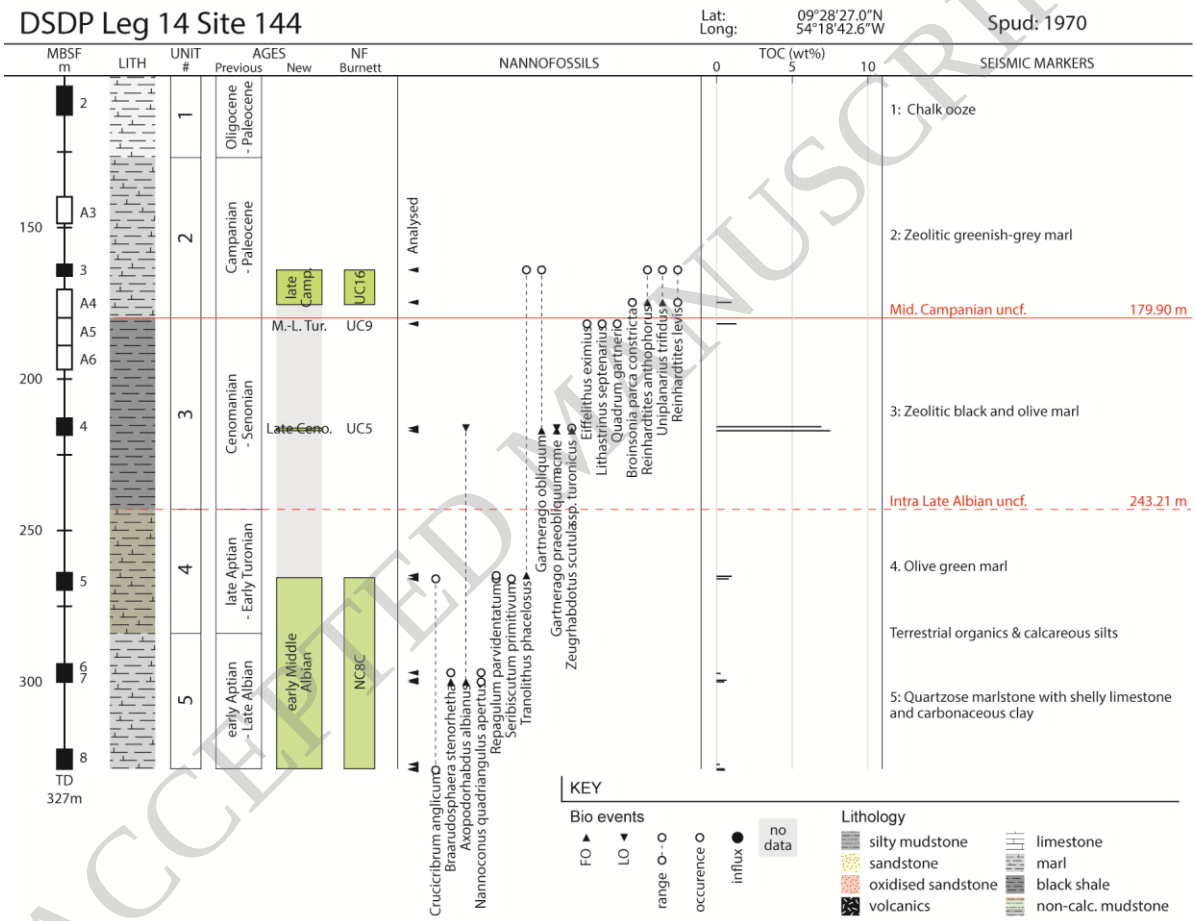

ACCEPTED MANUSCRIPT

Downloaded from http://pg.lyellcollection.org/ at University of Manchester, The John Rylands University Library on February 1, 2021

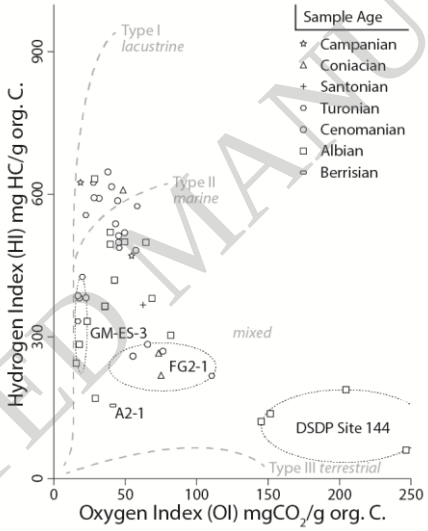

ACCEPTED MANUSCRIPT

Downloaded from http://pg.lyellcollection.org/ at University of Manchester, The John Rylands University Library on February 1, 2021

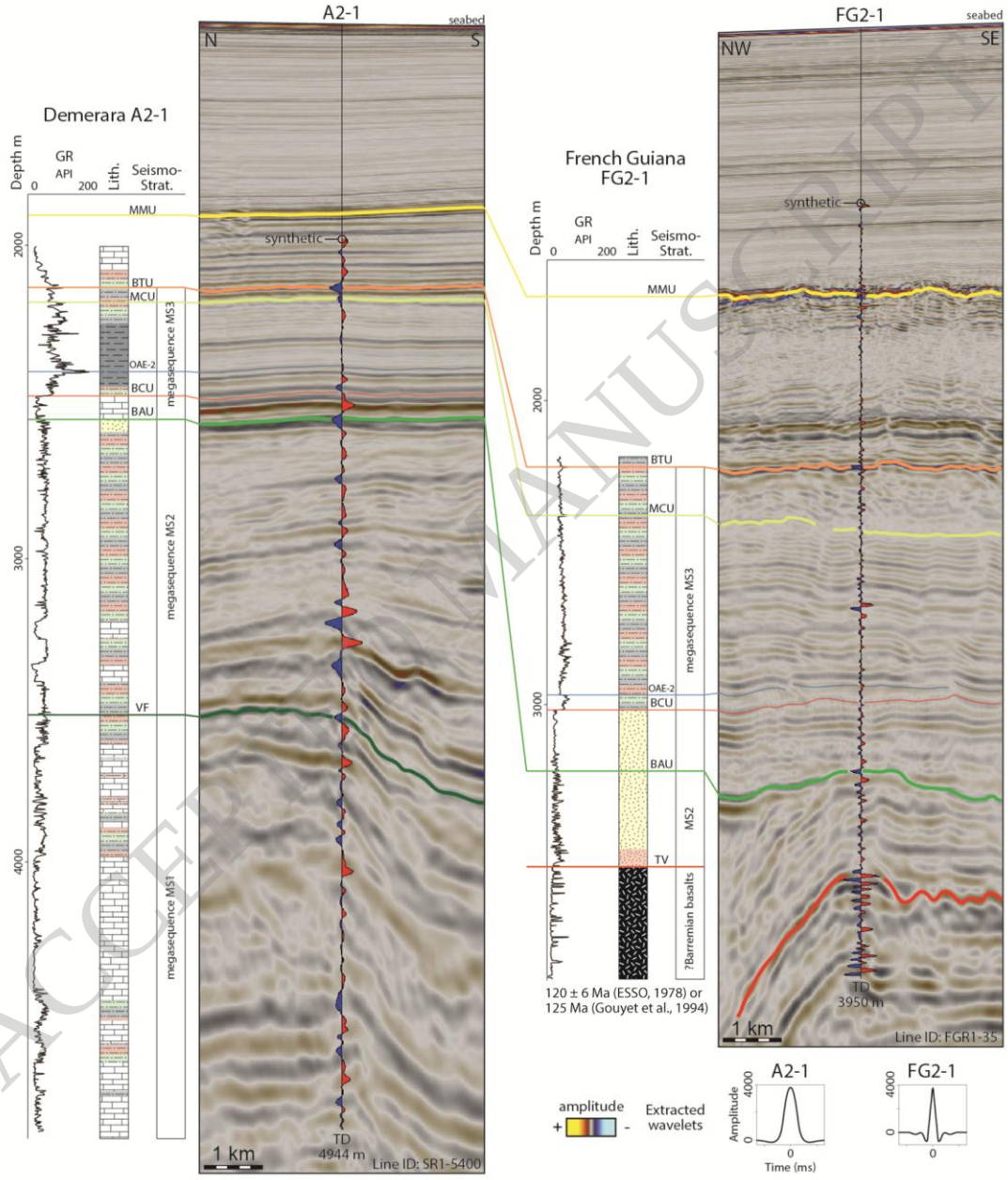

ACCEPTED MANUSCRIPT

Downloaded from http://pg.lyellcollection.org/ at University of Manchester, The John Rylands University Library on February 1, 2021

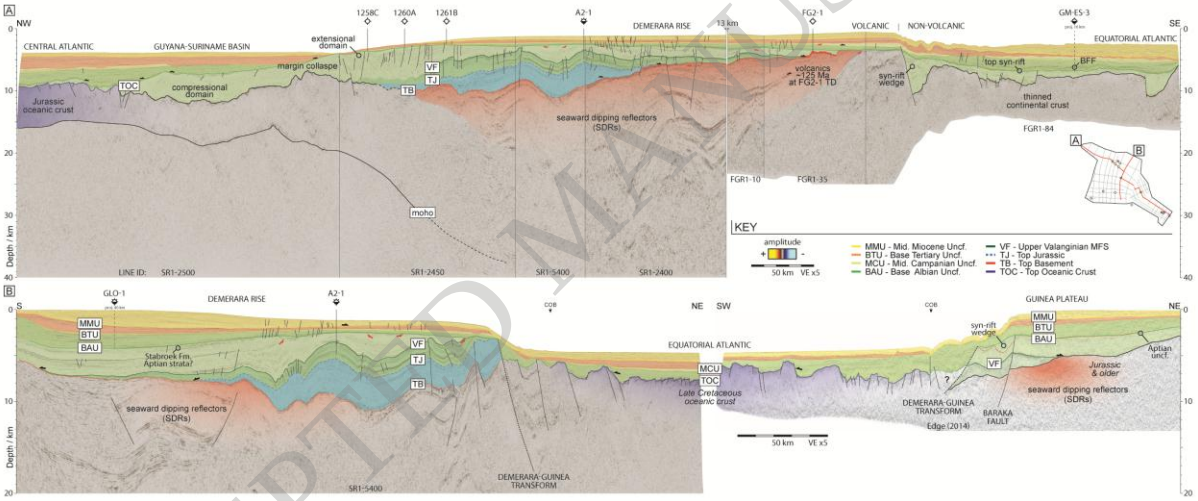

ACCEPTED MANUSCRIPT

Downloaded from http://pg.lyellcollection.org/ at University of Manchester, The John Rylands University Library on February 1, 2021

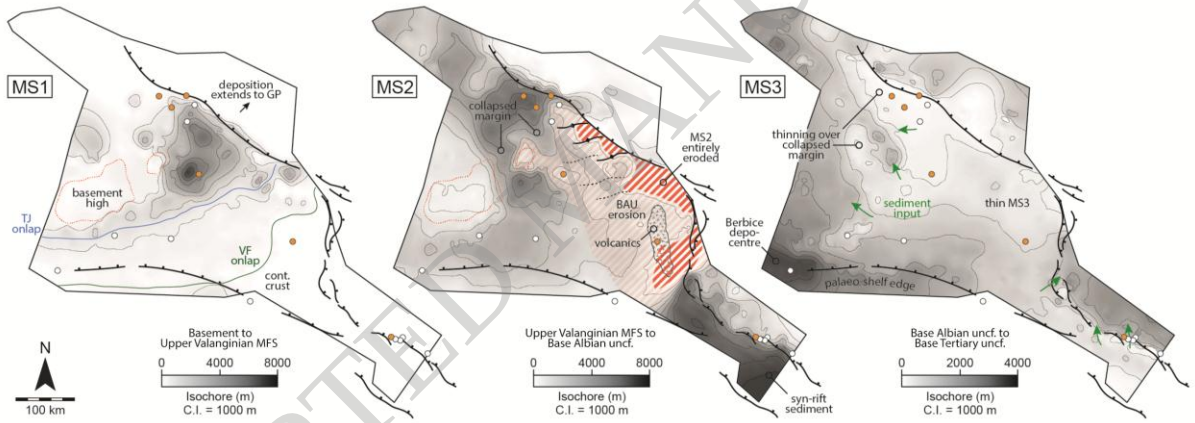

ACCEPTED MANUSCRIPT

Downloaded from http://pg.lyellcollection.org/ at University of Manchester, The John Rylands University Library on February 1, 2021

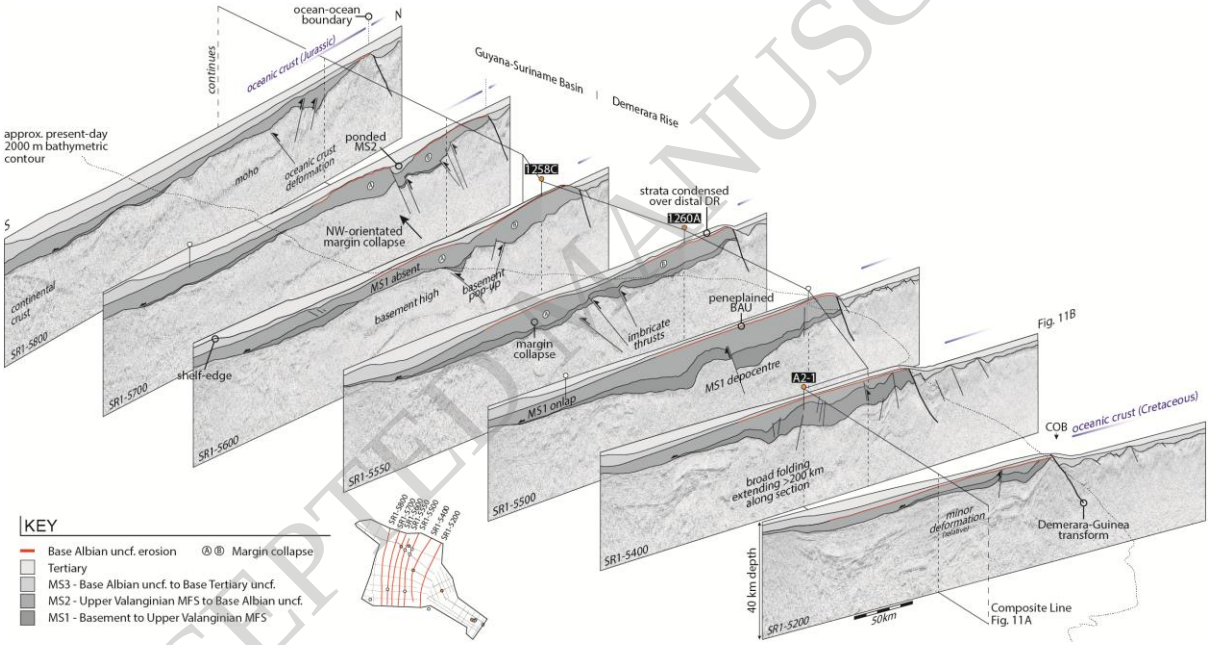

ACCEPTED MANUSCRIPT

Downloaded from http://pg.lyellcollection.org/ at University of Manchester, The John Rylands University Library on February 1, 2021

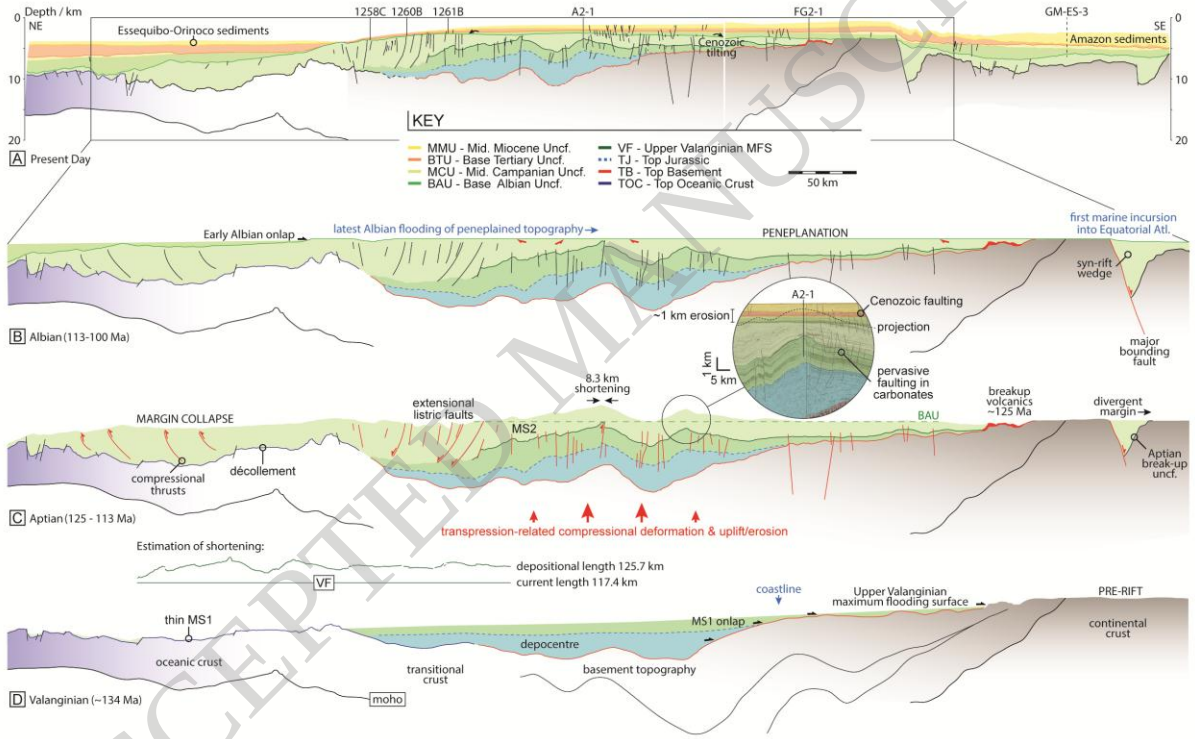

ACCEPTED MANUSCRIPT

Downloaded from http://pg.lyellcollection.org/ at University of Manchester, The John Rylands University Library on February 1, 2021

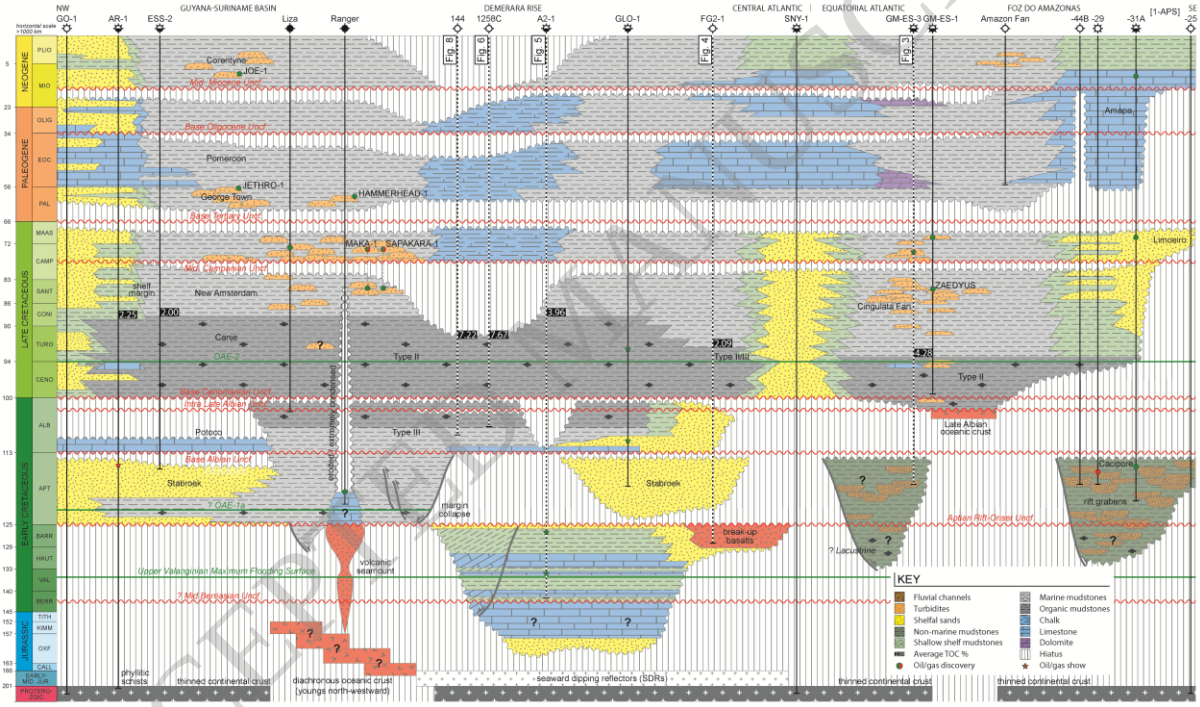

ACCEPTED MANUSCRIPT

Downloaded from http://pg.lyellcollection.org/ at University of Manchester, The John Rylands University Library on February 1, 2021

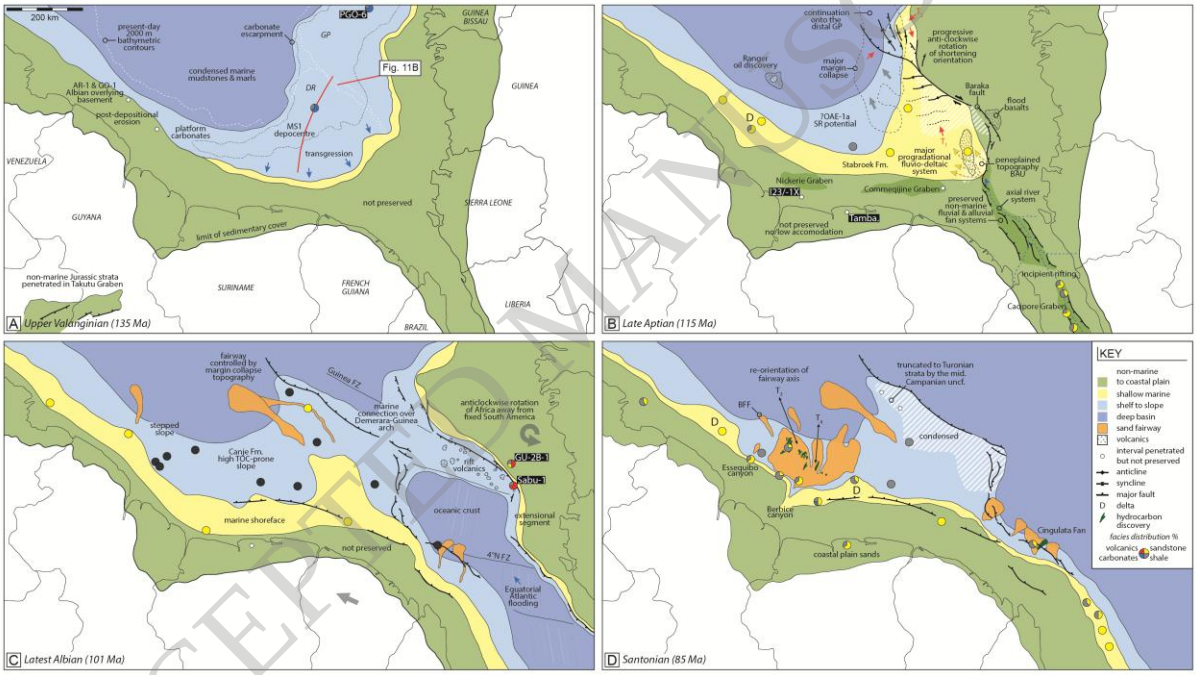

ACCEPTED MANUSCRIPT